Energy Storage Materials 61 (2023) 102883

Contents lists available at ScienceDirect

Energy Storage Materials

journal homepage: www.elsevier.com/locate/ensm

Deep Learning Framework for Lithium-ion Battery State of Charge Estimation: Recent Advances and Future Perspectives

Jinpeng Tian [a], Cheng Chen [a,*], Weixiang Shen [b], Fengchun Sun [a], Rui Xiong [a,*]

[a] Department of Vehicle Engineering, School of Mechanical Engineering, Beijing Institute of Technology, Beijing 100081, China
[b] School of Science, Computing and Engineering Technologies, Swinburne University of Technology, Hawthorn, Victoria 3122, Australia

ARTICLE INFO

Keywords:
Lithium-ion battery
State of charge
Deep learning
Battery management

ABSTRACT

Accurate state of charge (SOC) constitutes the basis for reliable operations of lithium-ion batteries. The deep learning technique, a game changer in many fields, has recently emerged as a promising solution to accurate SOC estimation, particularly in the era of battery big data consisting of field and testing data. It enables end-to-end SOC estimation using raw battery operating data as input for various battery chemistries under different operating conditions. This article first identifies SOC estimation problems and introduces a general framework of deep learning-based SOC estimation and then reviews the recent applications of deep learning in SOC estimation with a focus on the model structure. Three kinds of prevalent deep neural networks (DNNs) are explained, including the fully connected neural network, recurrent neural network and convolutional neural network. Furthermore, advanced applications such as transfer learning and the combination of deep learning with other methods are discussed. Finally, challenges and future opportunities regarding data collection, model development and real-world applications are systematically examined to give insights into this area. Apart from SOC estimation, the present study is also promising to inspire advances in other battery management tasks.

1. Introduction

1.1. Background of SOC estimation

Lithium-ion batteries are dominant electrochemical energy storage devices, whose safe and reliable operations necessitate intelligent state monitoring [1–3]. In particular, state of charge (SOC), which is defined as the ratio of the available capacity to the maximum capacity, is a fundamental state to ensure proper battery management [4]. However, as only current, voltage and sometimes surface temperature of lithium-ion batteries are measurable, SOC cannot be directly measured but needs to be estimated. As demonstrated in Fig. 1, conventional battery SOC estimation methods generally fall into three categories, namely Ampere-hour counting, model-based methods and filter-based methods [5,6].

The Ampere-hour counting method assumes an accurate initial SOC. Then, the SOC variation is computed by integrating the current over time to determine the present SOC. As an open-loop method, its performance is susceptible to the limited current sampling accuracy, leading to gradual degradation of the estimation accuracy. A systematic analysis by Zheng et al. [5] revealed that the estimation error can reach 5% given a current drift of 5 mA in 100 hours for a 100-Ah battery system. Besides, the information on battery voltage characteristics is ignored.

Model-based methods are a more prevalent choice. Such methods draw on voltage models to establish the link between voltage signals and SOC [7]. It is widely accepted that open circuit voltage (OCV) is a reliable indicator of SOC. Therefore, the SOC can be estimated by identifying OCV with a voltage model, as demonstrated by Xiong et al. [8] and Meng et al. [9]. Commonly used models include electrochemical models [10–12] and equivalent circuit models (ECMs) [13,14].

The filter-based methods combine the above two kinds of methods to form a closed-loop estimation. They predict SOC through Ampere-hour counting which is then fed into a voltage model to simulate voltage response. The error between the measured and simulated voltage is used as feedback to correct the SOC prediction. The feedback gain can be computed using various filters [15] and observers [16].

The above three kinds of methods have received immense attention. Many review articles have systematically discussed these methods [5,7] which generally face the following critical challenges.

* Corresponding Authors: School of Mechanical Engineering, Beijing Institute of Technology, No. 5 South Zhongguancun Street, Haidian District, Beijing 100081, China, Tel./Fax: +86 (10) 6891−4070
E-mail addresses: chencheng@bit.edu.cn (C. Chen), rxiong@bit.edu.cn (R. Xiong).

https://doi.org/10.1016/j.ensm.2023.102883
Received 6 October 2022; Received in revised form 30 June 2023; Accepted 10 July 2023
Available online 11 July 2023

First, battery models play a critical role in model-based and filter-based methods. However, the application of battery models requires cumbersome parameterisation. Electrochemical models involve tens of parameters, some of which are confidential owing to commercial reasons, leading to difficulties in model parameterisation [17]. ECMs [14] and fractional order models (FOMs) [15] are relatively simpler and less accurate than electrochemical models, they also require time-consuming OCV tests to determine the OCV-SOC relationship.

Second, owing to the missing physics and incorrect assumptions during model development, battery models have shown limited accuracy at low temperatures [14] and in the low SOC region [18]. For instance, Liu et al. [18] have pointed out that the widely used single particle model (SPM) oversimplifies solid-state diffusion, giving rise to high errors at low SOCs. The error of the simulated voltage from the battery models can further negatively impact SOC estimation.

Third, SOC estimation accuracy deteriorates for lithium-ion batteries whose voltage is not sensitive to SOC variation. For example, $LiFeO_4$ batteries have a flat OCV-SOC relationship, which means that a slight OCV error can cause a high SOC estimation error [19]. Quantitative analysis by Zheng et al. [20] revealed that a 1 mV voltage simulation error can yield a 5% SOC estimation error in the presence of voltage plateaus. Li et al. [21] compared three kinds of state-of-the-art filter-based methods for SOC estimation of $LiFeO_4$ batteries, and the results show that the SOC error can reach up to 7.3%.

1.2. Deep Learning SOC estimation Framework

The limitations of existing SOC estimation methods motivate the battery community to develop more accurate and efficient SOC estimation methods. The fast development of artificial intelligence has accelerated the popularity of data-driven SOC estimation. Ng et al. [4] discussed the promising applications of machine learning in the estimation of SOC and state of health (SOH) for batteries. This work systematically reveals the advantages of machine learning techniques in the context of state estimation. The discussed machine learning techniques include linear regression, random forest, support vector machine, Gaussian processes and neural networks. Algorithm selection rules are proposed and the authors identify the importance of data collection for machine learning based methods. Since its publication in 2020, a large spectrum of machine-learning solutions emerged to address state estimation problems [22,23]. In general, owing to the broad topic of machine learning, the applications of deep learning are not discussed in depth. Besides, this work does not focus on a particular state. Recently, Luo et al. [24] attempts to explore the applications of deep learning in SOC and SOH estimation of lithium-ion batteries. They first analyse the ECMs and electrochemical models before discussing the promising capability of machine learning and deep learning for battery state estimation. Both review papers [4,24] insightfully demonstrate the importance of data-driven approaches, while the recent development trend of deep learning-based SOC estimation methods has not been analysed in depth.

Deep learning, represented by deep neural networks (DNNs), has become a game changer in many fields, such as computer vision and natural language processing [25]. As the DNNs can carry out end-to-end learning by automatically learning all steps between the initial input and the eventual output, the reliance on expert knowledge or feature engineering can be significantly eased. Recently, deep learning has spurred innovation in the field of battery management. Deep learning-based SOC estimation methods can directly map sampled battery operating signals (e.g., current and voltage) to SOC. Therefore, arduous battery modelling or feature engineering is no longer needed [26–28]. In addition, deep learning methods have high scalability, which allows training models based on large datasets coming from different types of batteries. In the era of big data where massive battery operating data are collected [29,30], deep learning methods become a promising alternative and are expected to bridge the gap between the surge of battery big data and the

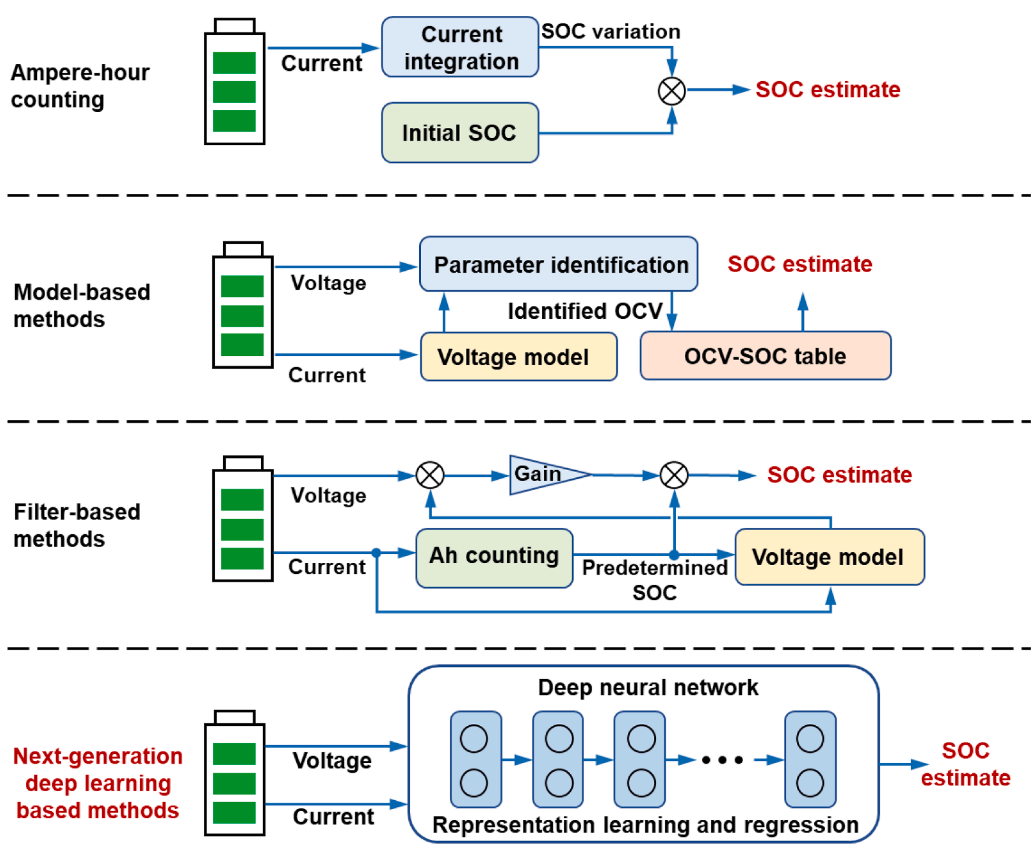

Fig. 1. Schematic diagrams of four kinds of SOC estimation methods.

limited learning ability of conventional SOC estimation methods. Recent studies have substantiated the efficacy of deep learning methods under various challenging conditions, even in the presence of low SOCs [31], low temperatures [32] and voltage plateaus [33,34].

This article aims to provide a comprehensive review of the applications of deep learning in battery SOC estimation. Challenges and future opportunities are also systematically analysed to advance next-generation battery state estimation. The methods discussed in this review are promising to be extended to other data-driven battery research, such as degradation diagnosis [35–37] and fault diagnosis [38,39].

1.3. Article organisation

The rest of the article is organised as follows. Section 2 formulates the SOC estimation problem and the typical deep learning-based solutions. Section 3 elaborates on various types of DNNs for SOC estimation and their corresponding examples. Section 4 discusses advanced applications of DNNs. Section 5 analyses the challenges faced by existing studies and also clarifies future research opportunities.

2. State of charge estimation and deep learning

2.1. State of charge estimation

As mentioned earlier, battery SOC is defined as

$$SOC_t = \frac{Q_t}{Q_{\max}} \tag{1}$$

where Q_t represents the available capacity at the time instant t and $Q_{\max}$ represents the maximum capacity, which can be obtained through measurement or estimation [40].

Since SOC is not directly measurable, a battery management system (BMS) attempts to use the sampled current, voltage and other signals (e.g., surface temperature) to determine SOC. As shown in Fig. 1, deep learning methods establish a nonlinear mapping between the measured signals and SOC in an end-to-end manner. Without losing generality, we take the most frequently used voltage and current data as an example. At the time instant t, the voltage and current sequences are collected in a window with the length of T, which are then fed into a DNN to estimate SOC:

$$\begin{cases} x_t = [V_t \quad I_t]^T \\ \hat{z}_t = f_{\text{DNN}}(x_{t-T+1:t}) \end{cases} \tag{2}$$

where V, I and $\hat{z}$ represent voltage, current and the SOC estimation result, respectively. $x_{t-T+1:t} = (x_{t-T+1}, x_{t-T+2}, \ldots, x_t)$ represents the input sequence. f_{DNN} stands for the mapping between the input and output.

2.2. Framework of deep learning based SOC estimation

In contrast to conventional model-based methods which establish the mapping by resorting to physics-based models, deep learning methods provide a convenient approach to learning the mapping from vast training data. Specifically, deep learning uses a deep structure to learn hierarchical representations from training data [25]. This process is generally fulfilled by neural networks because of their flexible structure. In general, the deep learning-based SOC estimation includes data generation, model development and model deployment as shown in Fig. 2.

Data generation: As a data-driven approach, DNNs rely on a training dataset to learn the mapping described in Eq. (2). A training dataset accommodates the voltage and current data collected from battery operations. The reference SOC is computed by resorting to Ampere-hour counting. In the context of battery testing, high-accuracy battery test equipment and a regulated testing environment can ensure accurate current sampling. In addition, the initial SOC can be accurately determined by fully charging/discharging the batteries to the upper and lower voltage limits, which correspond to the SOC of 100% and 0, respectively [5]. Then, the current and voltage data can be sliced together with reference SOC to support the supervised training of a DNN. The training data are expected to cover wide SOC ranges, and the current and voltage profiles are expected to reflect realistic battery usage. Existing training datasets can be classified into two types, namely static and dynamic datasets. The static dataset considers the battery SOC estimation under a controllable condition to rule out the impact of unseen current excitations. For instance, battery charging is controllable in many scenarios. In view of this, Tian et al. [33] investigated the SOC estimation during the constant-current constant-voltage (CCCV) charging, which is a prevalent battery charging protocol adopted in electric vehicles (EVs). A DNN was adopted to map the current and voltage sequence to the SOC according to Eq. (2). Once the SOC is estimated at the constant-current charging stage, the SOC is propagated based on Ampere-hour counting until the next charging stage. Hu et al. [34] extended this kind of method from the CCCV charging to additional four advanced charging protocols, including multistage constant current constant voltage (MCCCV), constant power constant voltage (CPCV), alternating current (AC) and pulse charging (PC). The results demonstrate the effectiveness of the DNN-based SOC estimation under various charging conditions.

The dynamic datasets represent more general cases where the batteries operate under dynamic current excitations. Such cases are prevalent in many new-energy energy storage scenarios, such as photovoltaic systems where energy generation and consumption are both dynamic

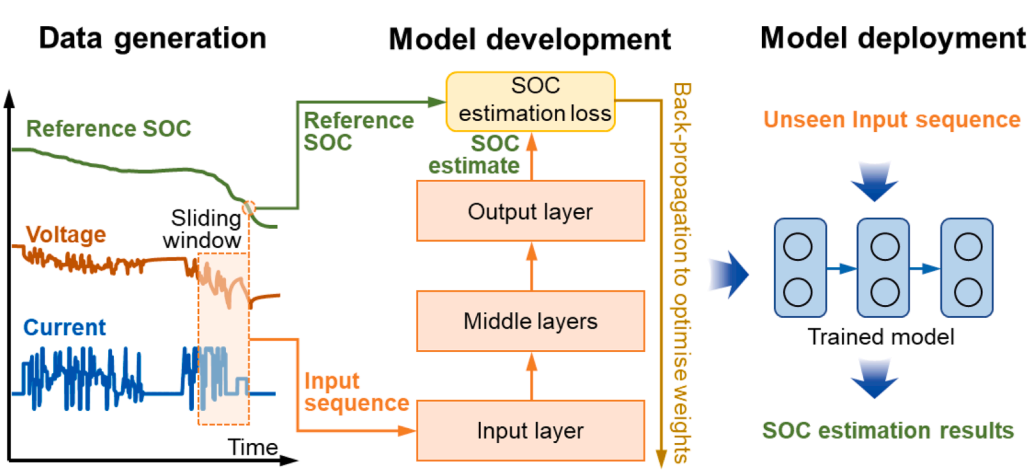

Fig. 2. Structure and training strategy of a deep neural network for SOC estimation.

[40]. In this regard, a variety of dynamic profiles have been imposed on batteries to simulate the dynamic discharge of batteries. There are a few open datasets that are publicly available, as summarised in Table 1. These datasets cover different battery materials, dynamic profiles and working conditions, which have supported the development and validation of many DNN-based SOC estimation methods. However, as the real-world profiles depend on factors such as driving habits, regions, and seasons, existing datasets based on standard driving profiles may not reflect real-world battery operations. Studies based on field data [29,41] are expected to advance the training and validation of deep learning-based SOC estimation.

It should be underlined that the two types of training datasets can cover different battery degradation levels to inform the DNNs with battery characteristics at different states. In this way, the DNNs are expected to estimate SOC at different ageing levels. Besides, the flexibility of DNNs allows us to integrate other battery states for estimation, such as the SOH. Detailed discussions of the joint estimation can be found in Section 5.2.3.

Model development: a DNN can be established to learn the mapping described in Eq. (2) from the training dataset. As shown in Fig. 2, a DNN consists of an input layer, multiple middle layers and an output layer. The stacked layers incorporate representation learning and sequential data regression, offering high flexibility in handling various types of data [46]. In this regard, the model performance heavily depends on the layer and model structures. In addition to the basic DNN with the fully connected layers, advanced layers with powerful feature extraction abilities have been developed by the deep learning community [25]. For example, the convolutional layer, inspired by findings in terms of biological vision, provides state-of-the-art performance for image processing. The recurrent neural network (RNN) layers can accommodate the sequence-dependent data and have demonstrated their efficacy for speech recognition. The working principles and applications of different types of DNNs are discussed in Section 3 to clarify their performance in terms of SOC estimation.

Once a DNN is developed, it is usually parameterised in a supervised fashion. Weights in each layer are optimised by minimising the discrepancy between the SOC estimate and experimentally obtained reference SOC:

$$\theta_{\mathrm{DNN}} = \operatorname{argmin} f_{\mathrm{loss}}(z, \hat{z}) \tag{3}$$

where z and $\hat{z}$ are the reference SOC and estimate, respectively. f_{loss} is the loss function measuring the difference between the estimation results and reference. In the context of battery SOC estimation, a variety of loss functions can be adopted, such as the mean squared error (MSE) [47] and mean squared error (MAE) [31]. The minimisation problem is addressed through backpropagation [48], i.e., parameters are updated using the following rule:

$$\theta_{\mathrm{DNN}} \leftarrow \theta_{\mathrm{DNN}} - \eta \frac{\partial f_{\mathrm{loss}}(z, \hat{z})}{\partial \theta_{\mathrm{DNN}}} \tag{4}$$

where η denotes a learning rate.

Model deployment: The trained DNN model can be deployed in a BMS to estimate SOC from pieces of voltage and current data. The estimation results can serve as the basis for other battery management tasks such as battery charging [49] and fault diagnosis [38].

Table 1
Public datasets containing dynamic profiles for SOC estimation.

Dataset	Battery type	Dynamic profiles	Temperature
[42]	Panasonic 18650PF	US06, HWFET, UDDS and LA92	-20°C~25°C
[43]	LG 18650HG2	US06, HWFET, UDDS and LA92	-20°C~40°C
[44]	Turnigy Graphene 5000mAh 65C cell	US06, HWFET, UDDS and LA92	-20°C~40°C
[45]	A123 $LiFePO_4$ battery	DST and FUDS	-10°C~50°C

3. Deep neural networks for SOC estimation

DNNs play a central role in deep learning-based SOC estimation methods with various types of layers. Among them, fully connected neural networks (FCNNs), RNNs and convolutional neural networks are widely accepted. This section provides a detailed discussion of their working principles and applications in SOC estimation.

3.1. Fully connected neural networks

The FCNN is one of the most prevalent DNNs, and its structure is shown in Fig. 3. In an FCNN, each neuron in one layer is connected to all neurons in the next layer. Accordingly, the output of the kth neuron in the lth layer is

$$y_k^{(l)} = f_{\mathrm{a}}\left(\sum_j w_{j,k}^{(l)} y_j^{(l-1)} + b_{j,k}^{(l)}\right) \tag{5}$$

where $y_k^{(l)}$ is the output of the kth unit in the lth layer, $w_{j,k}^{(l)}$ and $b_{j,k}^{(l)}$ are the weight and bias between the jth neuron in the (l-1)th layer and the kth neuron in the lth layer. $f_{\mathrm{a}}()$ denotes an activation function, such as the rectified linear unit (ReLU), which is expressed as $f_{\mathrm{a}}(x) = \max(x, 0)$.

As a basic DNN type, the effectiveness of FCNNs has been demonstrated by a few studies. For instance, Chemali et al. [50] developed a SOC estimation method based on an FCNN. In the proposed method, the present SOC is modelled as a function of the present voltage, current, temperature and the average current and voltage over 400 precedent time steps. The proposed method shows high accuracy under various temperatures. In a follow-up study by How et al. [51], the influence of the number of middle layers on SOC estimation was investigated. Their results show that deep FCNNs have improved modelling ability under unseen conditions but face overfitting risk. To reasonably determine hyperparameters, they proposed to use a backtracking search algorithm to optimise the number of neurons and learning rate during the model training stage [52].

The FCNNs have intrinsic limitations. First, the fully connected structure comprises a large number of parameters, especially when a long sequence is directly taken as input. This issue gives rise to high computational costs and overfitting risk. Besides, it can hardly process multivariate sequences unless the input data are flattened. Therefore, the fully connected structure can hardly be directly used to estimate battery SOC without condensing its input. More advanced DNN architectures have become the mainstream for SOC estimation.

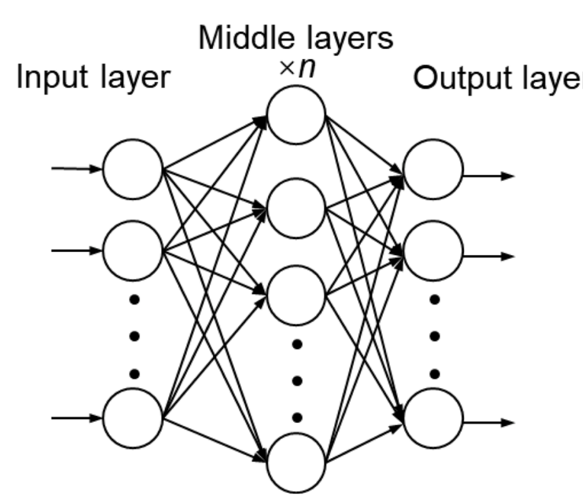

Fig. 3. Structure of a fully connected neural network.

3.2. Recurrent neural networks

3.2.1. RNN architecture and units

As the current and voltage signals are typically sampled as a time sequence, RNNs have been widely employed to estimate battery SOC to take advantage of their intrinsic capability of processing sequence-dependent data. Different from FCNNs where time dependency is not accommodated, in an RNN layer, a hidden state h is introduced to transfer information over time steps. For the sake of brevity, we use $x_{1:T} = (x_1, x_2, \ldots, x_T)$ to replace $x_{t-T+1:t}$ in Eq. (2), thus the SOC estimation can be rewritten as

$$\hat{z} = f_{\mathrm{DNN}}(x_{1:T}) \tag{6}$$

The RNN layer utilises a state to retain information regarding the input sequence, and this can be expressed as

$$h_t = f_{\mathrm{RNN}}(x_t, h_{t-1}) \tag{7}$$

where $h_t \in \mathbb{R}^D$ is a D-dimensional state vector, $x_t \in \mathbb{R}^M$ is an M-dimensional input vector. f_{RNN} denotes a nonlinear function described by an RNN unit.

As shown in Fig. 4, the simplest RNN has a sequential structure, which is given as

$$h_t = \tanh(w_h h_{t-1} + w_x x_t + b) \tag{8}$$

where $\tanh(x) = \frac{\exp(x)-\exp(-x)}{\exp(x)+\exp(-x)}$, $w_h \in \mathbb{R}^{D\times D}$ and $w_x \in \mathbb{R}^{D\times M}$ are two weight matrices. b is a bias matrix. After iteratively processing the entire input sequence, we obtain the last state vector h_T as a representation of the input sequence. Afterwards, the state vector h_T can be mapped to the target SOC:

$$\hat{z} = g(h_T) \tag{9}$$

where $g()$ denotes the nonlinear mapping between h_T and the SOC prediction result, which is usually modelled by a shallow FCNN [31].

The effectiveness of the RNN in SOC estimation is corroborated by a few studies. For example, Zhao et al. [53] proposed to use an RNN to obtain a vector representation of input sequence data to accomplish SOC estimation. Lipu et al. [54] applied RNN to the SOC estimation of two types of batteries, and the RNN hyperparameters (e.g. the number of neurons) were optimised by a firefly algorithm. The results indicate the superior performance of RNNs in comparison with FCNNs.

3.2.2. LSTM and GRU

Owing to the gradient vanishing and exploding problem, the basic RNN cannot deal with long input sequences. Advanced gated RNNs which have a superior ability to deal with long sequences have been proposed to address this issue, such as long short-term memory (LSTM) [55]. As shown in Fig. 5(a), the gate structure is introduced in an LSTM unit and two states are used to carry information across multiple time steps. The working principle of LSTM layers is detailed in supplementary note 1 and the reader is referred to [55].

By using the gate structure, the LSTM has high capability in processing long sequences, and it has been reported to demonstrate high accuracy in many fields, such as time series prediction [56], machine translation [57] and health prognosis [58,59]. However, its complex structure gives rise to high computational burdens. The gated recurrent unit (GRU) RNN [60,61] was proposed to balance the computational costs and accuracy. The GRU has comparable performance to the LSTM but lower computational costs, thanks to its simpler structure and fewer training parameters. See supplementary note 2 and the original research [55] for the working principles of GRU.

In the context of battery SOC estimation, LSTM-based RNNs have been frequently explored. Chemali et al. [62] and Yang et al. [32] developed an LSTM-based RNN to estimate battery SOC, respectively. Their validation results show that more LSTM neurons can lead to better estimation accuracy. Ma et al. [31] developed an LSTM-based RNN to simultaneously estimate battery SOC and state of energy (SOE). In their method, an LSTM layer is built followed by a dense layer to map its output to the two states. The training loss is the sum of MSEs of SOC and SOE estimation. Their validation results show that the LSTM can accurately estimate the two critical battery states at the same time. While the above methods are based on an empirical selection of hyperparameters, Ren et al. [63] adopted the particle swarm optimization (PSO) algorithm to search for five hyperparameters of the LSTM DNN, such as the neurons in the layer and initial learning rate. Besides, random noise was added to the input data to train the model, in order to improve the robustness under noisy conditions.

The GRU-based RNNs have also been widely studied for SOC estimation. In [64], the application of GRU on SOC estimation was investigated to take advantage of its efficiency and accuracy. A systematic investigation of the influence of the ambient temperature and model hyperparameters was carried out, and the authors concluded that the GRU achieves better performance compared with conventional model-based methods. Hannan et al. [65] developed a GRU model to estimate SOC with current, voltage and temperature sequences. A one-cycle learning rate policy was adopted to improve the DNN performance. Validation results demonstrate that the proposed method is more accurate and efficient than LSTM.

3.2.3. Stacked RNNs

The flexibility of the RNNs allows us to stack multiple layers to improve the learning capability. As shown in Fig. 6 (a), a stacked RNN uses multiple RNNs to process the input sequence, which is formulated as

$$h_t^{(i)} = \begin{cases} f\left(h_{t-1}^{(1)}, x_t\right) & \text{if} \quad i = 1 \\ f\left(h_{t-1}^{(i)}, h_t^{(i-1)}\right) & \text{else} \end{cases} \tag{10}$$

where $f()$ is the nonlinear function expressed by the RNN units such as LSTM and GRU. The superscript (i) denotes the ith RNN layer. By stacking more RNN layers, the RNN has enhanced learning capabilities.

In the context of battery SOC estimation, Yang et al. [66] built a deep LSTM model by stacking three LSTM layers. Hannan et al. [65] developed a two-layer GRU model. Their validation results show that deep

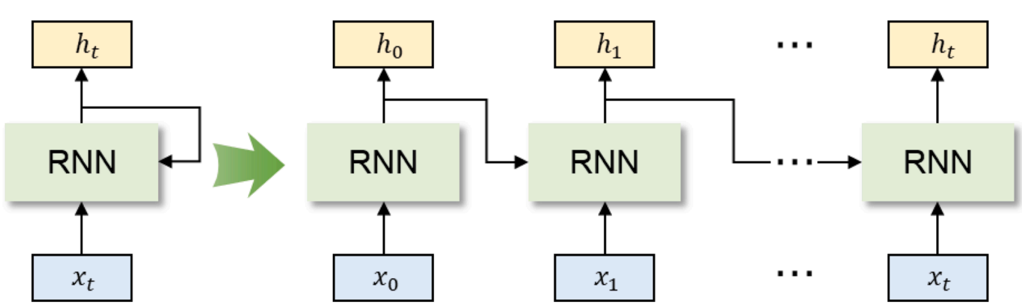

Fig. 4. Structure of an RNN layer.

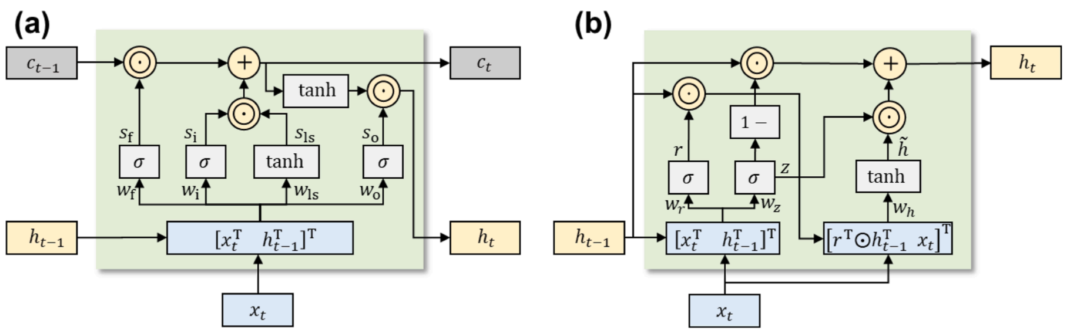

Fig. 5. Schematic diagrams of (a) LSTM and (b) GRU units.

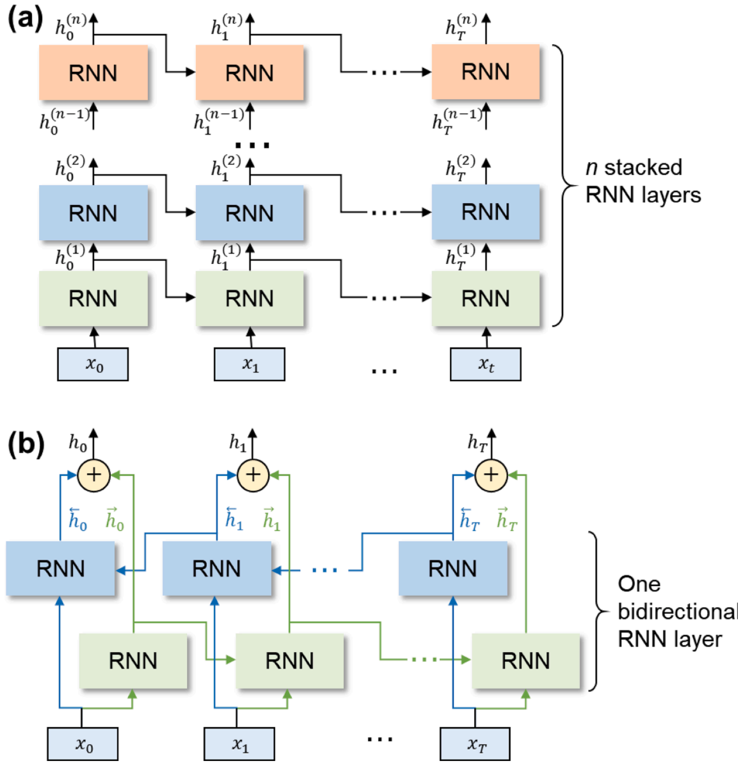

Fig. 6. Schematic diagrams of (a) stacked and (b) bidirectional RNNs.

RNNs with more than one layer have improved learning ability than those RNNs with only one layer. However, stacking more layers does not always give rise to accuracy improvement and may encounter the problem of overfitting, which limits the generalisation of a DNN to unseen inputs. Results from [67] show that a DNN with two layers possesses the best performance for the adopted dataset. In this regard, the number of layers can be considered as a hyperparameter to be determined through optimisation [63].

3.2.4. Bidirectional RNNs

In addition to the stacked RNN layers, the bidirectional architecture is also an attractive alternative to improve the learning ability of DNNs. As shown in Fig. 6(b), a bidirectional RNN layer scans its input sequence in both forward and backward directions. The generated feature vectors are then concatenated as the final one. Therefore, it can effectively extract temporal information from its input data. This process is mathematically expressed as

$$\overrightarrow{h}_t = f\left(\overrightarrow{h}_{t-1}, x_t\right) \tag{11}$$

$$\overleftarrow{h}_t = f\left(\overleftarrow{h}_{t+1}, x_t\right) \tag{12}$$

$$h_t = \overrightarrow{h}_t \oplus \overleftarrow{h}_t \tag{13}$$

where $\overrightarrow{h}$ and $\overleftarrow{h}$ are the forward and backward states, respectively. The symbol $\oplus$ denotes the element-wise sum of two vectors.

A bidirectional LSTM was utilised for SOC estimation in [67]. The experimental validation results confirm that the bidirectional LSTM outperforms the single-direction one. Similarly, Zhang et al. [68] applied this idea to the GRU layer and developed a bidirectional GRU model for SOC estimation. A Nesterov accelerated gradient algorithm was adopted to overcome the oscillation problem in the gradient descent process. Although high accuracy is obtained, the bidirectional RNNs have doubled the number of parameters, leading to high computational costs. This issue can be alleviated by optimising the model hyperparameters such as the number of layers and cells [63,69]. For instance, How et al. [69] carried out hyperparameter optimisation of various types DNNs through a Bayesian strategy. Their results show that the optimised bidirectional GRU model can achieve the highest accuracy with a relatively low computational cost.

3.2.5. Encoder-decoder architecture

The RNN can also serve as the output layer to generate a sequence as its input. In this regard, the sequence-to-sequence (seq2seq) model is widely used, as shown in Fig. 7. This model was originally proposed for national language processing, e.g., it can help translate one sentence into a different language.

In the seq2seq model, the encoder is first used to extract features from the input sequence:

$$h_T^{(E)} = f_{\mathrm{encoder}}(x_{1:T}) \tag{14}$$

where f_{encoder} represents the nonlinear function expressed by the encoder. $h_T^{(E)}$ is the last hidden state generated by the encoder. It is then repeated to form a sequence as the input of the decoder, and the output of the decoder is expressed as

$$h_t^{(D)} = f_{\mathrm{decoder}}\left(h_T^{(E)}, h_{t-1}^{(D)}\right) \tag{15}$$

where f_{decoder} represents the nonlinear function expressed by the decoder. $h_t^{(D)}$ is the state of the decoder RNN at the tth step, which is further mapped to the SOC estimation result:

$$\hat{z}_t = g\left(h_t^{(D)}\right) \tag{16}$$

where $g()$ represents the mapping function, which can be modelled by an FCNN.

Inspired by this, Ma et al. [70] developed a seq2seq model for SOC estimation. The encoder comprises an LSTM layer to process the input voltage and current sequence and outputs a feature vector. The following decoder also comprises an LSTM layer, which takes the feature vector as the input while outputting a SOC sequence. The authors also proposed a two-stage training strategy. In the first stage, the encoder is first trained in an unsupervised fashion by reconstructing the input. In this way, the encoder LSTM can learn how to process the input data. In the second stage, the decoder is concatenated to the pre-trained encoder to form the seq2seq model, which is trained using the input and the SOC sequences. In [71], Yang et al. developed a seq2seq model based on GRU. The spatial and temporal attention mechanisms are incorporated into the encoder and decoder, respectively, to improve the DNN performance. Their validation results show that the seq2seq model outperforms its counterparts without attention mechanisms under different dynamic profiles or temperatures.

3.2.6. Other advanced RNNs

In addition to the popular RNN variants such as the LSTM and GRU, some advanced variants of the RNN have been proposed to improve the performance of SOC estimation. For instance, the Independently recurrent neural network (IndRNN) [72] was employed in [73] for SOC estimation. The neurons in an IndRNN layer can connect across different layers but remain independent of each other. This feature allows the IndRNN to build a deep structure. In [74], a clockwork RNN [75] was utilised for the SOC estimation. The clockwork RNN divides a layer into a few modules, each of which is assigned a different clock period to model long-term dependencies. Both variants [73,74] have been experimentally demonstrated to outperform LSTM and GRU in terms of accuracy and training efforts, respectively.

3.2.7. Discussions

In summary, the structure of RNNs makes them a favourable choice for SOC estimation, in which the input data are multi-variate sequences. Validations have demonstrated their high accuracy for different battery chemistries under various conditions. In particular, LSTM and GRU are two representative RNNs whose applications have attracted much attention. However, the present RNNs take a universal form for various problems and do not take into account the characteristics of batteries. For instance, the voltage and current sequences are treated equally in the input sequence. In reality, the current is subject to battery usage while the voltage is deemed as the response. However, existing RNN applications have no mechanism to represent this relationship.

Furthermore, the present RNNs cannot consider the time dependency in the SOC estimation results, which may lead to high fluctuations in the SOC estimation even at two adjacent moments. In reality, the SOC variation is governed by the Ampere-hour counting [47], which is neglected by the RNN-based SOC estimation methods.

In addition, although techniques such as cross-validation are generally adopted in the training phase [76], the RNNs face the risk of overfitting. Xi et al. [77] investigated the SOC estimation of $LiFeMgO_4$ batteries using an RNN variant. They revealed that overexcited neurons can give rise to the issue of overfitting. An empirical method to detect this issue was proposed by monitoring the power spectrum of neurons. However, validations on other variants of RNNs need further investigation.

3.3. Convolutional neural networks

3.3.1. Basics of convolutional neural networks

Convolutional neural networks (CNNs) are another prevalent deep learning algorithm. Since it was proposed by LeCun [78], it has been rapidly applied in many fields such as image and video processing. In the field of battery state estimation where sequential data are generally studied, the 1D CNN has become an attractive choice [79]. Different from the RNNs, the 1D CNN layers can process input sequences using a set of kernels in parallel. As demonstrated in Fig. 8(a), each kernel utilises a sliding window to sample from the input sequence and compute

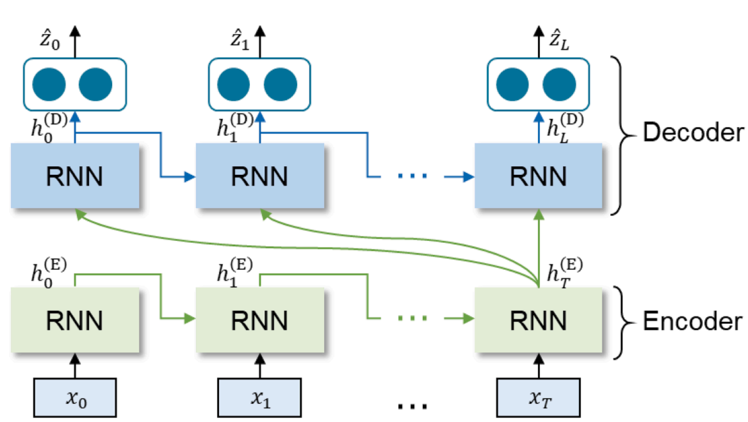

Fig. 7. Schematic diagram of the seq2seq structure.

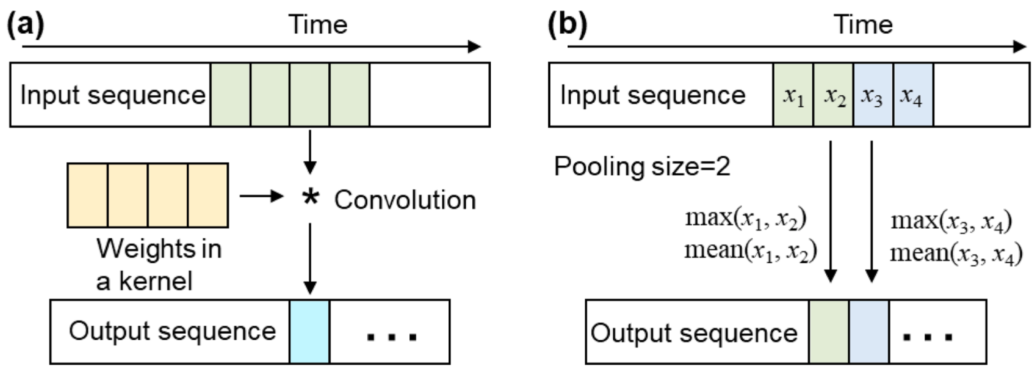

Fig. 8. Schematic diagram of (a) a 1D convolutional kernel and (b) an example of pooling.

the weighted sum as the element of the output sequence. The output sequences of each kernel are stacked as the output of a 1D CNN layer.

The pooling layer provides a down sampling method to extract features from a convolutional layer, the commonly used down-sampling method includes max pooling and average pooling. The max pooling layer conducts down-sampling by computing the maximum in a given window. An example of the mean and maximum pooling is shown in Fig. 8(b). The pooling layer can reduce computational costs and help alleviate over-fitting by reducing the dimension of input data. Mathematical expressions of the CNN and pooling layers can be found in Supplementary note 3.

3.3.2. *Applications of CNNs in SOC estimation*

When it comes to battery SOC estimation, Hannan et al. [80] developed a CNN in which four blocks comprising convolutional and max-pooling layers are stacked to process the input current, voltage and temperature sequence, followed by a fully connected layer to map the extracted features to the SOC estimation. Besides, a learning rate optimisation method was exploited to improve the training. The authors systematically compared the developed CNN with RNNs. Their results reveal that CNN outperforms RNNs in terms of accuracy and computational efficiency.

In addition to the basic CNN, more advanced CNN variants have been applied to SOC estimation. For example, Hu et al. [76] and Guo et al. [81] devised the temporal convolutional neural network (TCN) [82,83] for SOC estimation. The TCN was designed with two structural improvements for processing temporal sequences, namely dilated causal convolution [84] and residual connection [85]. As illustrated in Fig. 9(a), the dilated causal convolution ensures that the present output comes from only previously observed inputs. Moreover, the receptive field can be exponentially enlarged when stacking more layers, which is conducive to the effective utilisation of historical data. In addition, the residual connection is employed to stabilise deeper and larger TCNs. As demonstrated in Fig. 9(b), this is implemented by adding shortcut connections across layers. Given an input x, residual connection transforms the task of learning a mapping $H(x)$ to learn the residual $F(x){:=}H(x)$-x, thereby alleviating the difficulties in optimising deep DNNs.

It should be noted from Section 3.3.1 that a CNN kernel utilises a fixed kernel to extract and condense information, which limits the time resolution of the CNN. However, the flexibility of the DNNs can accommodate different time scales in the input data. Bhattacharjee et al. [86] proposed a multi-branch CNN architecture for SOC estimation. In the developed CNN, three CNN branches consist of convolutional layers, pooling layers and fully connected layers. Due to different kernel sizes in convolutional layers, the branches can capture long and short-term temporal dependencies in the input data. The authors also investigated two methods to merge the output of three branches and experimentally determined the best choice. Experimental results confirmed the reliable prediction results under common and noisy conditions. Fig. 10 gives a visual comparison between the single-branch and multi-branch CNNs.

In addition to the 1D CNNs, 2D CNNs have been reported in [87] for SOC estimation. In this method, the 1D voltage, current and temperature sequences are reshaped into 2D matrices, which are further processed using a 2D CNN. Interestingly, the validation results show the 2D CNN outperforms the 1D counterpart. The authors ascribe the improved accuracy to the wider receptive field of 2D convolution than that of the 1D convolution. However, the transformation is intuitive, without in-depth validations on different hyperparameter settings. Advanced signal processing techniques such as Wavelet transform have been demonstrated to effectively convert 1D time series to 2D time-frequency maps. Since the generated time-frequency maps can reflect the time-frequency properties of the original time series, the performance of CNNs can be effectively improved, as demonstrated by an example of fault diagnosis [88]. As batteries operating signals typically cover a wide spectrum of timescales [89], the integration of signal processing techniques and DNNs is promising to benefit the accuracy of state estimation.

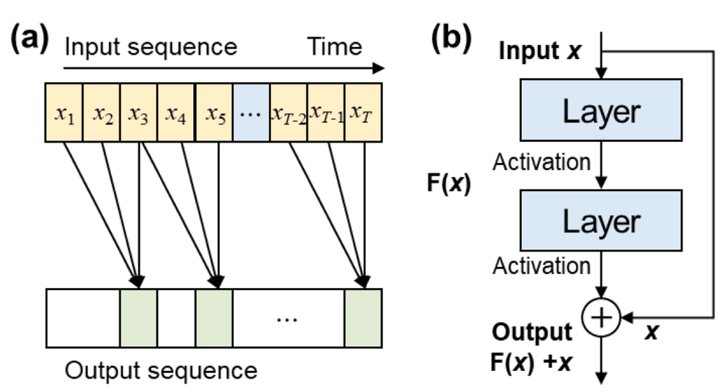

Fig. 9. (a) Dilated causal convolution with a filter size of 3. (b) A residual block.

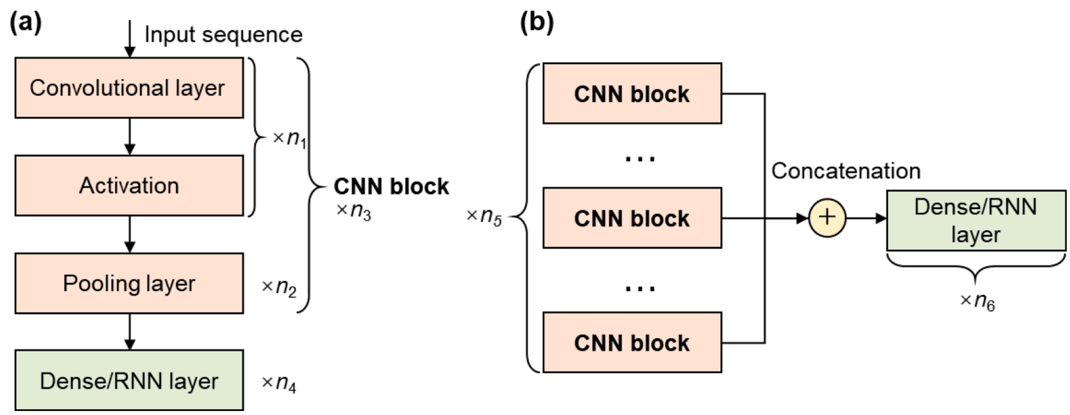

Fig. 10. Schematic diagram of (a) single-branch and (b) multi-branch CNNs. $n_1 \sim n_6$ are integers indicating that layers/blocks can be repeated multiple times.

3.3.3. Discussions

The examples discussed above confirmed the capability of CNNs to provide efficacious SOC estimation. These advantages enable the CNNs to use few parameters to efficiently process long sequences. In principle, CNNs have several advantages making them attractive solutions for SOC estimation. First, unlike RNNs which process data in sequence, convolutions can be carried out in parallel, making the CNNs efficient in processing long input sequences. Second, without relying on a recurrent architecture, CNNs overcome a major drawback of RNNs, i.e., gradient vanishing. In addition, the receptive field size of CNNs can be flexibly adjusted using parallel branches [86] or stacked layers [81] to accommodate different applications.

However, CNNs still have some limitations for the task of SOC estimation. Similar to the RNNs, CNNs cannot explicitly distinguish the voltage and current sequences. In addition, basic CNNs are insensitive to the order of the input, thereby cannot capture the time dependency in input sequences. The incorporation of CNNs and RNNs is promising to achieve a balance between efficiency and accuracy [76]. For example, in the SOC estimation method proposed by Hu et al. [76], TCN [82,83] is used to extract features among the input sequence, which are further fed into an LSTM to capture the temporal dependency. Validations using the EV driving profiles under different temperatures confirm the high accuracy of the TCN-LSTM model over independent TCN and LSTM models at the expense of increased computational burden. Similar architectures have also been reported in [33,90,91].

4. Advanced applications of deep neural networks for SOC estimation

In addition to the basic applications which use the DNNs to map battery operating data to SOC, some recent studies have contributed to advanced applications of DNNs to enhance their SOC estimation performance. They are transfer learning and the combination of DNNs with other methods. In the following sections, we analyse these two paradigms.

4.1. Transfer learning

Behind the success of deep learning-based SOC estimation, there is a critical assumption regarding the training data. It is usually assumed that the training and testing samples are drawn from the same distribution. However, owing to the inconsistency in cell characteristics and variations in battery operating conditions, the assumption may not strictly hold, leading to the “dataset shift” issue [92,93] and jeopardising estimation performance. A straightforward solution is to collect more data to bridge the gap between the training dataset and real-world samples. However, this solution may incur prohibitive costs and in some cases, it may be not practical for research purposes. An alternative to circumvent this issue is transfer learning, whose effectiveness has been demonstrated in the fields of computer vision [94] and machine fault diagnosis [95].

Mathematically speaking, transfer learning defines a source domain to represent a primary training dataset, which can be expressed as

$$D^{(s)} = \left\{\left(x_i^{(s)} \quad y_i^{(s)}\right)\right\}_{i=1}^{n^{(s)}} x_i^{(s)} \in X^{(s)}, y_i^{(s)} \in Y^{(s)} \tag{17}$$

where $D^{(s)}$ denotes the source domain, $x_i^{(s)}$ and $y_i^{(s)}$ are the input and label of the ith sample in the source domain, respectively. $X^{(s)}$ and $Y^{(s)}$ the collections of $x_i^{(s)}$ and $y_i^{(s)}$, respectively. $n^{(s)}$ is the total number of samples in the source domain.

On the other hand, a target domain $D^{(t)}$ is defined as

$$D^{(t)} = \left\{\left(x_i^{(t)} \quad y_i^{(t)}\right)\right\}_{i=1}^{n^{(t)}} x_i^{(t)} \in X^{(t)}, y_i^{(t)} \in Y^{(t)} \tag{18}$$

where $x_i^{(t)}$ and $y_i^{(t)}$ are the input and label of the ith sample in the target domain, respectively. $X^{(t)}$ and $Y^{(t)}$ the collections of $x_i^{(t)}$ and $y_i^{(t)}$, respectively. $n^{(t)}$ is the total number of samples in the target domain. The target domain represents the case where a trained model is intended to be used.

The source and target domains have different probability distributions but we hope to develop a DNN to fulfil the regression task in $D^{(t)}$:

$$\hat{y}_i^{(t)} = f_{\mathrm{DNN}}\left(x_i^{(t)}\right) \tag{19}$$

As $D^{(s)}$ and $D^{(t)}$ follow different distributions, it is expected that the DNN trained on $D^{(s)}$ to obtain f_{DNN} may not achieve satisfying results. On the other hand, the target domain $D^{(t)}$ may consist of a few samples to support developing f_{DNN}. Consequently, it is necessary to take advantage of both $D^{(s)}$ and $D^{(t)}$ with transfer learning. As shown in Fig. 11, two widely used transfer learning methods for SOC estimation are fine-tuning and domain adaptation.

4.1.1. Fine-tuning

Fine-tuning is a two-stage approach to carrying out transfer learning. A DNN is firstly trained on the source domain using sufficient training samples. The trained DNN can be used as the starting point of the DNN for the target domain as it learns to process the input sequence to extract underlying features and establish the mapping between the features and SOC estimates. To let the pre-trained DNN adapt to the target dataset, a few new samples in the target dataset can be utilised to fine-tune parameters in certain layers in a supervised manner. The fine-tuning method is schematically shown in Fig. 11(a).

The effectiveness of the fine-tuning method has been illustrated in many SOC estimation studies [33,86,96]. For example, it was adopted for SOC estimation of different battery types in [33]. Firstly, a DNN

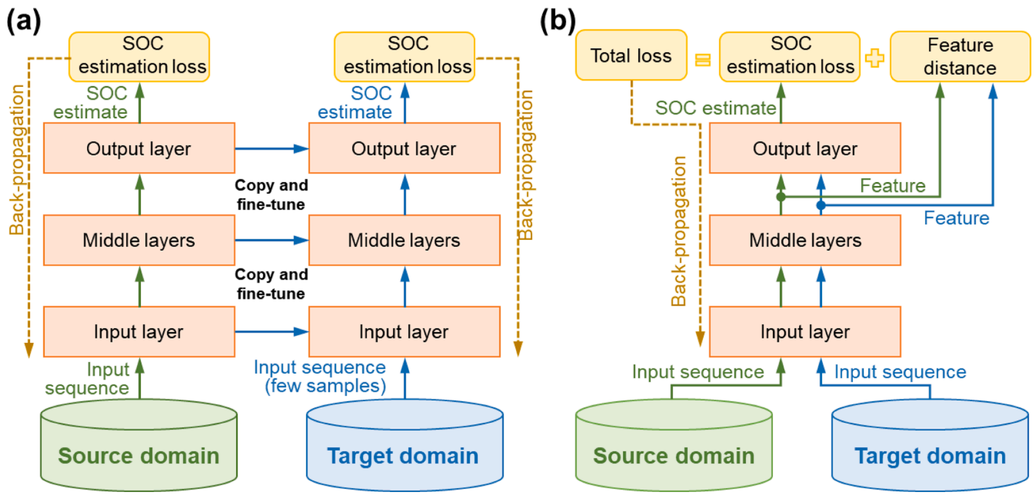

Fig. 11. Schematic diagram of two transfer learning strategies. (a) fine-tuning and (b) domain adaptation.

comprising convolutional layers, a GRU layer and a fully-connected layer is developed, which accepts the constant-current charging data as input for SOC estimation. A pre-trained DNN based on 20 Ah batteries is employed to initialize a DNN for 27 Ah batteries. Experimental results show that fine-tuning is faster and more accurate than developing a DNN from scratch. In [86], a three-branch CNN was developed for SOC estimation, transfer learning is implemented by fine-tuning three CNN branches while freezing the dense layers after concatenation. The effectiveness of this method was substantiated based on two battery chemistries. Liu et al. [96] further proposed a rolling learning strategy to guide fine-tuning. The dense layer in an LSTM DNN is fine-tuned once sufficient training data are online collected. The proposed method enables to update of the SOC estimation online using a minor amount of training data.

4.1.2. Domain adaptation

The domain adaptation method can be used when the labels (i.e., actual SOC) are not available in the target domain. It does not rely on labelled samples from the target dataset to fulfil transfer learning. Instead, it learns domain-invariant features from the source and target datasets, and then resorts to the source domain labels to develop the mapping between features and estimation results. As demonstrated in Fig. 11(b), the domain adaptation method typically considers two loss functions [93,97,98]. In this method, nonlinear mapping is constructed using DNNs to map the samples of the source domain and the target domain from their independent feature spaces to a shared feature space. Then, the distribution difference between the sample features of the source domain and the target domain is computed using the similarity measurement functions, such as the maximum mean discrepancy (MMD) [99,100] and Wasserstein distance [101].

Afterwards, the nonlinear mapping parameters are updated reversely by resorting to convex optimization theory to minimize the feature distribution difference, so that it can extract features with similar distribution from the samples of the source domain and target domain. The extracted features can then be used to train a regressor to implement regression. After the feature distribution is adapted, the target domain and the source domain have similar feature distributions. Therefore, the regressor trained by the samples from the source domain can assist with the prediction task of the target domain. Consequently, the overall training loss can be formulated as

$$J_{\text{total}} = J_{\text{SOC}} + \lambda J_{\text{D}} \tag{20}$$

where J_{SOC} is the SOC estimation loss, J_{D} is a loss to describe the feature distance, and λ is a weight to regulate domain adaptation.

Bian et al. [91] investigated the domain adaptation method for SOC estimation. They developed SOC estimation models using three types of batteries. Data collected from one type of battery is used as the source domain while data from the other two types of batteries are used as the target domain. A DNN comprising convolutional and LSTM layers is constructed, and the MMD distance between features extracted from the source and target domains is calculated. In their method, features extracted from multiple layers are aligned to improve the transfer learning accuracy. The ultimate training loss comprises the MMD at multiple layers and SOC estimation loss on the source and target domains. A comparative study based on three open datasets corroborates the superior accuracy over fine-tuning method. However, this study requires the labels of samples in the target domain, and further validation of unsupervised domain adaptation is preferable. Oyewole et al. [102] proposed a transfer learning-based SOC estimation method to cope with the discrepancy between cells. In the proposed method, an LSTM model is first trained on a source domain. Afterwards, further training is conducted on the target domain by using fine-tuning and MMD-based loss.

4.1.3. Discussions

In summary, existing transfer learning techniques have achieved impressive performance by alleviating the reliance on training data. The above-mentioned examples illustrate generalisable SOC estimation for different operating profiles, battery degradation levels, and even battery chemistries. However, a few underlying challenges need to be overcome before applying present transfer learning techniques to industrial SOC estimation. First, although the demand for training data is dramatically reduced, the present transfer-learning applications assume a specific target domain. Methods with higher generality to unseen conditions are expected for real-world SOC estimation. In addition, the reliability of transfer learning needs further exploration. The issue of "negative transfer" may harm the performance of SOC estimation models given a low similarity between the source and target domains [94].

4.2. Combination of DNNs with other methods

4.2.1. Combination of DNNs and Ampere-hour counting

The combination of DNNs with other methods aims to overcome the intrinsic limitations of DNNs by resorting to other modelling techniques. For example, in view of the "dataset shift" issue caused by inconsistent discharging profiles for DNN training and application, Tian et al. [33] proposed a method to combine DNN-based SOC estimation with Ampere-hour counting. As the charging protocols are usually controllable, DNN is only employed to calibrate the initial SOC of the Ah counting using a 10-min charging data piece as the input. Afterwards, Ah counting can be used to calculate SOC until the next charging process. Zheng et al. [5] analysed the error propagation of the Ah counting method and pointed out that SOC calibration should be performed every 7 days. In reality, battery charging would be more frequent, thereby stable SOC estimation can be ensured by the combination of DNN and Ah counting. The validation results show that the SOC estimation error can be restricted to 2.03% even in the presence of voltage plateaus of LFP batteries. In a follow-up study by Hu et al. [34], this method was further validated based on five state-of-the-art charging protocols at different temperatures. The evaluation on the input window size reveals that data collected in 90 s are enough to make accurate SOC estimation. Hence, the data storage and computational efforts can be reduced. However, this method is designed for batteries with controllable charging processes. For batteries subject to uncertain charging and discharging in solar or wind power generation systems, further validation is needed.

The filter-based method (Fig. 1) provides an adaptive solution to incorporate the DNNs and Ampere-hour counting. Eq. (2) implies that the DNN-based SOC estimation is an open-loop method, whose reliability might be negatively affected by factors such as noise. Note that the SOC estimation results at two subsequent moments are independent (i.e., $\widehat{z}_{k-1}$ and $\widehat{z}_k$ come from $x_{k-m:k-1}$ and $x_{k-m+1:k}$, respectively), the Ampere hour counting can be introduced to form a closed-loop estimation framework:

$$\begin{cases} z_{c,k} = z_{c,k-1} + \dfrac{\Delta t \eta}{Q_{\max}} I_{k-1} + w_{k-1} \\ \widehat{z}_k = z_{c,k} + v_k \end{cases} \tag{21}$$

where Δt is the sampling interval. η is the coulombic efficiency, and it approximates 1 for lithium-ion batteries. $z_{c,k}$ denotes the closed-loop SOC estimation result. The SOC estimation result from the DNN $\widehat{z}_k$ is considered the actual measurement of the SOC. w and v are the process and measurement noise, respectively. Filters or observers can be adopted to formulate an online closed-loop estimation, and the overall closed-loop framework is plotted in Fig. 12. For instance, a basic Kalman filter was adopted in [33] for this purpose. The results show that this framework can ensure reliable SOC estimation in the presence of random noise or abrupt disturbances. An LSTM DNN combined with an unscented Kalman filter (UKF) was proposed in [32] to improve estimation performance at different temperatures. However, it can be observed that Eq. (21) is a typical linear system, and the application of high-order nonlinear filters might lead to additional costs.

4.2.2. Combination of DNNs and physics-based models

In most studies regarding deep learning-based SOC estimation, the current and voltage data are directly mapped to the SOC, as described by Eq. (2). Fruitful and informative data can contribute to effective SOC estimation. Motivated by this, researchers have attempted to augment the input data or training samples to improve the SOC estimation performance.

Battery modelling studies have revealed that battery voltage characteristics exhibit multi-scale behaviours [103]. For instance, OCV changes slowly while voltage drop across internal ohmic resistance changes instantly as battery current varies. Moreover, SOC is a monotonic function of OCV while it is not sensitive to internal ohmic resistance. Given this, [47] employed a Thevenin model and extended Kalman filter (EKF) to decouple the battery voltage into physically meaningful subsequences, including OCV, polarisation voltage and Ohmic response. The decoupled voltage sequences were then fed into LSTM models for SOC estimation. Validation results confirm this method can improve the estimation accuracy for DNNs with different architectures. Both the Thevenin model and EKF are mature tools for online implementation, therefore this method is simple to implement. Yu et al. [104] designed a simplified electrochemical model to extract electrochemically meaningful variables from battery operating data to augment the input of an LSTM model. The impact of variable combinations was analysed to maximise the model performance. Apart from the model-based approach to decouple voltage data, Cheng et al. [105] proposed using wavelet transformation to decompose input voltage and current sequences into a series of wavelets of different frequencies. An FCNN was then developed to map the decomposed signals to SOC estimation results. Their validation results show this method can enhance SOC estimation accuracy at a small amount of the increased calculation cost.

The other type of data augmentation is to increase the number of samples that can be used to train DNNs. DNNs are a data-hungry machine learning framework, their training process requires a large number of samples. Otherwise, they may face the risk of overfitting. While the collection of experimental data for model training is a costly task, generating synthetic battery operating data by resorting to battery models is an effective alternative. Motivated by this, Ragone et al. [106] developed an electrochemical battery model to generate a large spectrum of training data to train the LSTM as well as another two machine learning algorithms for SOC estimation. This can alleviate the overfitting issue and support the development of larger DNNs. However, the trained SOC estimation models were not further validated with experimental data. Similar ideas have been reported by Dubarry et al. [107,108], who developed synthetic battery degradation datasets covering OCV curves with different electrode degradation levels and battery operating conditions.

4.2.3. Discussions

Although DNNs are a flexible solution that significantly advances the state estimation of batteries, their ability is restricted by training data. The examples discussed above demonstrate that the combination of DNNs and some simple methods (e.g., Ampere-hour counting and online model identification) can further boost the estimation performance with little additional computational costs. This fact implies that pure data-driven methods are not the optimal choice, and it is essential to deepen our understanding of battery characteristics when designing DNNs for state estimation tasks.

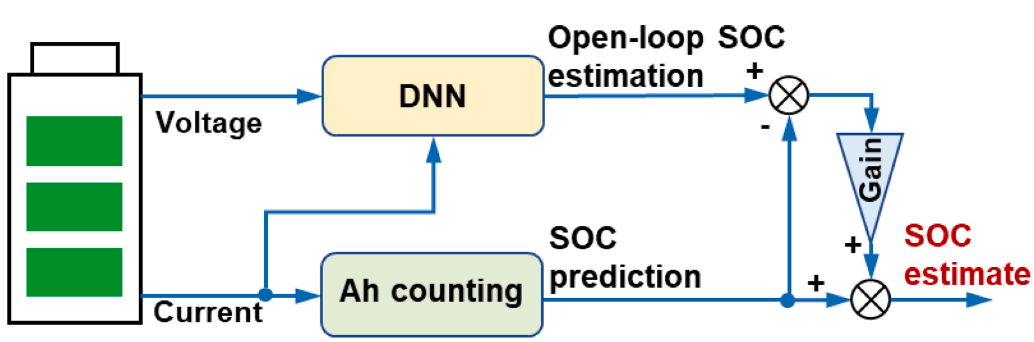

Fig. 12. Closed-loop SOC estimation incorporating DNN-based SOC estimation and Ampere-hour counting.

5. Challenges and opportunities

The review of deep learning-based SOC estimation in the previous sections indicates fast development in this area. However, there exist a few challenges to be addressed in the future. In this section, we categorise these challenges into the aspects of data, method and applications, as shown in Fig. 13. Furthermore, future research opportunities to address these challenges are systematically analysed.

5.1. Data collection for advanced SOC estimation

One of the most significant challenges for deep learning-based SOC estimation is the limited training data. Despite the DNNs are flexible enough to establish a high-dimensional mapping between battery operating data and SOC, the present SOC estimation studies are generally based on small experimental datasets obtained from standard EV driving profiles, as exemplified by Table 1. In reality, battery operations are highly dependent on many factors such as regions and driver habits. This issue is compounded by varying battery operating conditions, such as the ambient temperature.

There are two promising solutions to this issue. First, field data are valuable for model development and evaluation. Existing studies regarding battery fault diagnosis [109], degradation prediction [26] and EV driving pattern analysis [29] have demonstrated the effectiveness of data-driven methods assisted with field data. However, the sampled field data may have the deficiencies such as missing data or data with low sampling resolution [41]. More importantly, as batteries are not frequently fully charged or discharged and the data sampling accuracy is limited in most real-world applications, it is challenging to obtain data sequences with SOC labels. As a result, self-supervised [110] and semi-supervised [111,112] methods are required to make full use of such unlabelled data. Transfer learning discussed in Section 4.1 provides another solution to this problem. Using battery operating data of different cells and even different chemistries to assist with the DNN training process can help reduce the dependence on data of specific batteries.

In the case where field data are not available for model development, the combination of accurate battery models is an alternative to generate high-quality training data with labels. As discussed in Section 4.2.2, a few studies [106,107] have attempted to adopt a model-based approach to generate synthetic data to train DNNs. Mature tools such as the Python battery mathematical modelling (PyBaMM) project [113] provide a set of open-source electrochemical models for data generation. This allows the simulation of both voltage and temperature responses under various dynamic profiles. Besides, electrochemical models can provide valuable information regarding the internal states of batteries, such as the concentration of lithium ions in electrodes, giving deeper insights into battery state estimation. Furthermore, the emerging concept of battery "digital twin" [28,114] provides a virtual substitute for a real battery. It constitutes a promising tool to relax the requirement for training data. On the other hand, DNNs also have the ability for data generation. In [115], an encoder-decoder model was proposed to predict battery charging curves using one curve as its input. Thus, battery testing data can be augmented. In this regard, a combination of physical models and data-driven approaches to boost the training data is a promising solution to relax the requirement in terms of training data. An obstacle that needs to be noticed is the intrinsic gap between simulated and experimental data. Due to the assumptions in model development, models cannot accurately reflect battery characteristics. Transfer learning-based model training approaches are promising to surmount this obstacle. The DNNs trained using synthetic data will still need rigorous experimental validation.

5.2. Model development

5.2.1. Interpretability

Another challenge regarding SOC estimation with deep learning is interpretability. Although high accuracy has been achieved even for various battery chemistries, the end-to-end modelling using DNNs hinders the explanation of the prediction results. As a consequence, researchers and engineers cannot judge if a DNN can perform reliably under unseen conditions. The machine learning community has endeavoured to address this issue by designing explainable deep learning methods. Methods such as deep Taylor decomposition [116] and feature visualization [117] have been successfully introduced to the field of battery life prediction to indicate how the input is processed to make predictions. In comparison to the prediction of battery degradation, the SOC estimation needs to be performed in real time and faces the

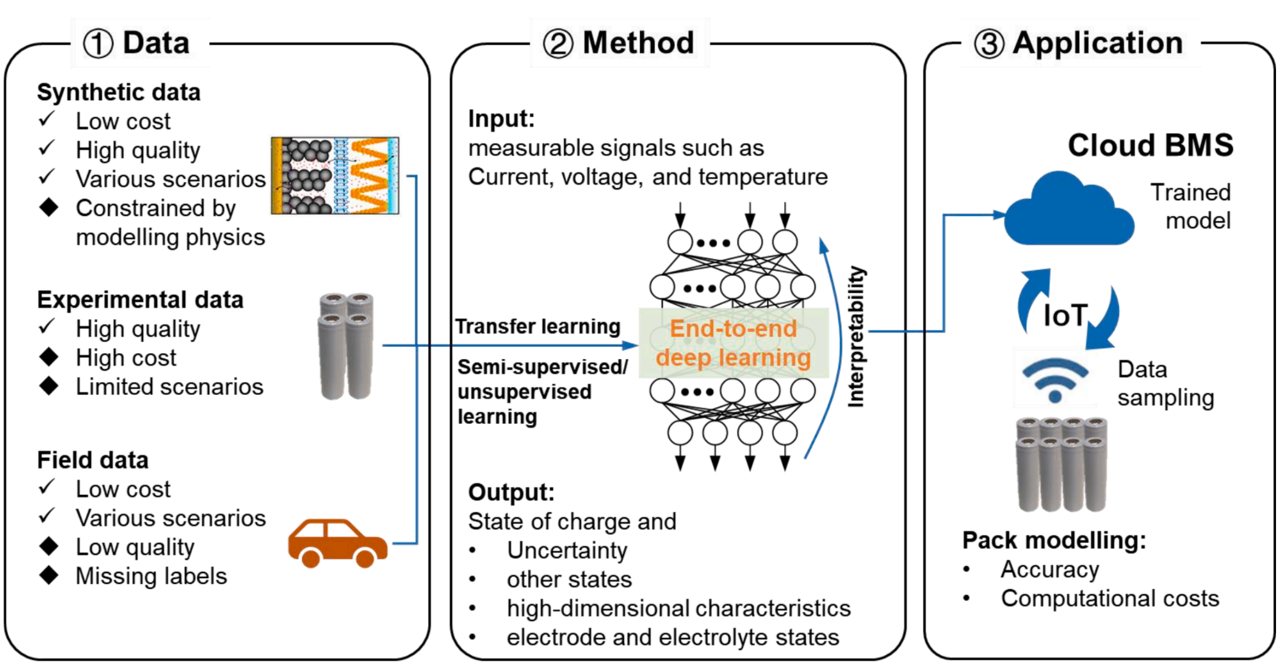

Fig. 13. Challenges and opportunities regarding data collection, deep learning models and their applications.

challenge caused by dynamic working conditions. These facts necessitate the online examination of the SOC estimation results.

5.2.2. Uncertainty estimation

At present, most studies are only concerned about the accuracy of the estimation results on specific test datasets, while neglecting the quantification of estimation uncertainty. However, only providing point SOC estimation results without indicating confidence jeopardises the application of DNNs in real-world applications as unreliable SOC estimates can hardly ensure the reliability of the subsequent battery management tasks.

Since batteries work in highly variable conditions, factors such as unexpected faults and noise can be detrimental to SOC estimation [81, 118,119]. In addition, Reza et al. [120] revealed that the incorporation of battery systems and new energy resources can significantly give rise to uncertain battery usage. Therefore, it is urgent to quantify the estimation uncertainty of battery states. Two types of uncertainty exist for DNN-based estimation [121], namely epistemic uncertainty and aleatoric uncertainty. The former refers to the uncertainty caused by the lack of knowledge and it can be alleviated by training the model with additional relevant training data. The latter can describe the inherent stochasticity of the observations. Therefore, uncertainty estimation can not only flag unreliable predictions but also alert model calibration when detecting the lack of knowledge. Some promising uncertainty estimation methods can be investigated in the future, particularly ones that can be applied to different DNN architectures, such as Monte-Carlo dropout [122], ensemble learning [123] and bootstrapping [124].

5.2.3. Joint estimation of multiple states

SOC is a fundamental state reflecting the remaining capacity in a battery. Its variation is highly correlated with other states. The high flexibility of DNNs allows us to simultaneously estimate multiple states, thereby saving computational costs. Ma et al. [31] revealed that a single LSTM DNN can simultaneously estimate SOC and SOE using voltage and current sequences as input. In [125], a CNN was trained using charging curves collected over battery life to simultaneously estimate the maximum and remaining capacities from short-term charging data. The estimation results can be used to define battery SOH and SOC, which are two states of different time scales. Given random charging data collected in 400 s, the CNN can estimate the maximum and remaining capacities with an error of 12.68 mAh for 740-mAh batteries. Interestingly, the results demonstrate that the simultaneous estimation of two states outperforms the individual state estimation, which can be attributed to the attention focus provided by multi-task learning [126]. Therefore, simultaneous estimation of relevant states is conducive to deep learning-based state estimation.

The estimation of battery states has also been extended to predict its high-dimensional characteristics. In [35], four electrode ageing parameters were predicted by feeding partial charging data into a CNN to reflect battery electrode degradation. More importantly, the prediction results can be used to reconstruct battery OCV curves at different ageing levels. This study shortens the time-consuming OCV tests (i.e., ~20 h for a current rate of 1/20 C) to a short-term daily charging. The reconstructed OCV curves can be used as the basis of battery modelling. In a follow-up study [127,128], data-driven prediction of entire charging curves was carried out using pieces of charging data as input. Battery states such as SOC, SOE and SOH can be derived as a function of charging voltage accordingly. Even impedance spectra can be predicted using charging data or short-term pulse data to describe the frequency-domain battery characteristics [129–131]. Therefore, the hardware and sampling requirements [132–135] can be significantly alleviated. These studies highlight that reconstructing battery working characteristics with deep learning can effectively address battery state estimation problems.

Monitoring the states of individual electrodes can provide deeper insights into battery states. Lin [136] developed an LSTM model to estimate anode potential using cell voltage, current and SOC as input. The validation results confirm the high accuracy of the proposed method with the RMSE<3.84 mV. In [137], the output of the LSTM was extended to plenty of electrochemical variables, including the average and surface lithium-ion concentration at electrodes, electrolyte concentration, electrode and electrolyte potentials while only the current, voltage and temperature are used as input. These studies confirm that DNNs are scalable to predict a variety of battery internal states using full-cell signals, but they were trained and validated using synthetic data generated by an electrochemical model. Their real-world applications require experimental results from three-electrode batteries, as demonstrated by studies in [138] and [139]. A comprehensive state estimation framework is expected to use battery operating data to reflect multiple battery characteristics with smart sensing techniques [140–142], which coincides with the aim of the battery "digital twin" [28,114,143].

5.3. Application in real-world battery management systems

The boosting of deep learning applications in battery SOC estimation necessitates more advanced BMSs. Although existing BMSs with microcontrollers [15] can hardly support the computation of DNNs for SOC estimation, advanced cloud BMSs [28] are promising to serve as the platform. Such cloud BMSs are scalable to accommodate complex DNNs. For example, a cloud BMS, together with the internet of things (IoT) has attracted much attention. Li et al. [144] developed a cloud BMS prototype to run a model-based SOC and SOH estimation method. The current and voltage data of the tested batteries sampled by a slave BMS are sent to the cloud via IoT. The state estimation was then carried out in a cloud BMS. A similar cloud BMS prototype has also been reported by Mondal et al. [145].

Modelling each cell in a battery pack independently will inevitably increase the computational cost of the battery pack [146]. To alleviate this issue, modelling a battery pack as a whole has been widely used in many BMS products [5]. On the other hand, representative batteries can be selected from a battery pack and their states are monitored to reflect the states of other batteries in the pack [147–150]. Nevertheless, few researchers have investigated the computational and data storage costs of DNNs in the context of a battery pack. Methods like data compressing [151] are promising to alleviate the efforts for achieving efficient state estimation.

In summary, the recent advances in deep learning provide an opportunity to design next-generation state estimation algorithms. This work provides a comprehensive understanding of deep learning methods and their applications in SOC estimation. We hope it can spur the development of efficient and reliable battery management systems.

CRediT authorship contribution statement

Jinpeng Tian: Methodology, Funding acquisition, Writing – original draft. **Cheng Chen:** Writing – review & editing. **Weixiang Shen:** Writing – review & editing, Supervision. **Fengchun Sun:** Writing – review & editing, Supervision. **Rui Xiong:** Conceptualization, Funding acquisition, Writing – review & editing.

Declaration of Competing Interest

The authors declare that they have no known competing financial interests or personal relationships that could have appeared to influence the work reported in this paper.

Acknowledgments

This work was supported by the National Key R&D Program of China (2021YFB2402002), the National Natural Science Foundation of China (52207229 and 52277213) and the China Postdoctoral Science Foundation (BX2021035 and 2022M710379).

Supplementary materials

Supplementary material associated with this article can be found, in the online version, at doi:10.1016/j.ensm.2023.102883.

References

[1] M. Anderman, The challenge to fulfill electrical power requirements of advanced vehicles, J. Power Sources. 127 (2004) 2–7, https://doi.org/10.1016/j.jpowsour.2003.09.002.
[2] Y. Qin, X. Chen, A. Tomaszewska, H. Chen, Y. Wei, H. Zhu, Y. Li, Z. Cui, J. Huang, J. Du, X. Han, L. Lu, B. Wu, K. Sun, Q. Zhang, M. Ouyang, Lithium-ion batteries under pulsed current operation to stabilize future grids, Cell Reports Phys. Sci. 3 (2022), 100708, https://doi.org/10.1016/j.xcrp.2021.100708.
[3] H. He, F. Sun, Z. Wang, C. Lin, C. Zhang, R. Xiong, J. Deng, X. Zhu, P. Xie, S. Zhang, Z. Wei, W. Cao, L. Zhai, China's battery electric vehicles lead the world: achievements in technology system architecture and technological breakthroughs, Green Energy Intell. Transp 1 (2022), 100020, https://doi.org/10.1016/j.geits.2022.100020.
[4] M. Ng, J. Zhao, Q. Yan, G.J. Conduit, Z.W. Seh, Predicting the state of charge and health of batteries using data-driven machine learning, Nat. Mach. Intell. 2 (2020) 161–170, https://doi.org/10.1038/s42256-020-0156-7.
[5] Y. Zheng, M. Ouyang, X. Han, L. Lu, J. Li, Investigating the error sources of the online state of charge estimation methods for lithium-ion batteries in electric vehicles, J. Power Sources. 377 (2018) 161–188, https://doi.org/10.1016/j.jpowsour.2017.11.094.
[6] M.A. Hannan, M.S.H. Lipu, A. Hussain, A. Mohamed, A review of lithium-ion battery state of charge estimation and management system in electric vehicle applications: Challenges and recommendations, Renew. Sustain. Energy Rev. 78 (2017) 834–854, https://doi.org/10.1016/j.rser.2017.05.001.
[7] R. Xiong, J. Cao, Q. Yu, H. He, F. Sun, Critical Review on the Battery State of Charge Estimation Methods for Electric Vehicles, IEEE ACCESS 6 (2018) 1832–1843, https://doi.org/10.1109/ACCESS.2017.2780258.
[8] H. He, R. Xiong, H. Guo, Online estimation of model parameters and state-of-charge of LiFePO4 batteries in electric vehicles, Appl. Energy. 89 (2012) 413–420, https://doi.org/10.1016/j.apenergy.2011.08.005.
[9] J. Meng, D.I. Stroe, M. Ricco, G. Luo, M. Swierczynski, R. Teodorescu, A novel multiple correction approach for fast open circuit voltage prediction of lithium-ion battery, IEEE Trans. Energy Convers. 34 (2019), https://doi.org/10.1109/TEC.2018.2880561.
[10] X. Han, M. Ouyang, L. Lu, J. Li, Simplification of physics-based electrochemical model for lithium ion battery on electric vehicle. Part II: Pseudo-two-dimensional model simplification and state of charge estimation, J. Power Sources. 278 (2015) 814–825, https://doi.org/10.1016/j.jpowsour.2014.08.089.
[11] C. Lin, A. Tang, J. Xing, Evaluation of electrochemical models based battery state-of-charge estimation approaches for electric vehicles, Appl. Energy. 207 (2017) 394–404, https://doi.org/10.1016/j.apenergy.2017.05.109.
[12] L. Xu, X. Lin, Y. Xie, X. Hu, Enabling high-fidelity electrochemical P2D modeling of lithium-ion batteries via fast and non-destructive parameter identification, Energy Storage Mater 45 (2022) 952–968, https://doi.org/10.1016/j.ensm.2021.12.044.
[13] X. Hu, S. Li, H. Peng, A comparative study of equivalent circuit models for Li-ion batteries, J. Power Sources. 198 (2012) 359–367, https://doi.org/10.1016/j.jpowsour.2011.10.013.
[14] X. Lai, Y. Zheng, T. Sun, A comparative study of different equivalent circuit models for estimating state-of-charge of lithium-ion batteries, Electrochim. Acta. 259 (2018) 566–577, https://doi.org/10.1016/j.electacta.2017.10.153.
[15] R. Xiong, J. Tian, W. Shen, F. Sun, A Novel Fractional Order Model for State of Charge Estimation in Lithium Ion Batteries, IEEE Trans. Veh. Technol. 68 (2019) 4130–4139, https://doi.org/10.1109/TVT.2018.2880085.
[16] Z. Wei, C. Zou, F. Leng, B.H. Soong, K.-J. Tseng, Online Model Identification and State-of-Charge Estimate for Lithium-Ion Battery With a Recursive Total Least Squares-Based Observer, IEEE Trans. Ind. Electron. 65 (2018) 1336–1346, https://doi.org/10.1109/TIE.2017.2736480.
[17] W. Li, Y. Fan, F. Ringbeck, D. Jöst, D.U. Sauer, Unlocking electrochemical model-based online power prediction for lithium-ion batteries via Gaussian process regression, Appl. Energy. 306 (2022), 118114, https://doi.org/10.1016/j.apenergy.2021.118114.
[18] M. Ouyang, G. Liu, L. Lu, J. Li, X. Han, Enhancing the estimation accuracy in low state-of-charge area: A novel onboard battery model through surface state of charge determination, J. Power Sources. 270 (2014) 221–237, https://doi.org/10.1016/j.jpowsour.2014.07.090.
[19] K. Zhang, R. Xiong, Q. Li, C. Chen, J. Tian, W. Shen, A novel pseudo-open-circuit voltage modeling method for accurate state-of-charge estimation of LiFePO4 batteries, Appl. Energy. 347 (2023), 121406, https://doi.org/10.1016/j.apenergy.2023.121406.
[20] Y. Zheng, M. Ouyang, L. Lu, J. Li, X. Han, L. Xu, H. Ma, T.A. Dollmeyer, V. Freyermuth, Cell state-of-charge inconsistency estimation for LiFePO4 battery pack in hybrid electric vehicles using mean-difference model, Appl. Energy. 111 (2013) 571–580, https://doi.org/10.1016/j.apenergy.2013.05.048.
[21] J. Li, J.Klee Barillas, C. Guenther, M.A. Danzer, A comparative study of state of charge estimation algorithms for LiFePO4 batteries used in electric vehicles, J. Power Sources. 230 (2013) 244–250, https://doi.org/10.1016/j.jpowsour.2012.12.057.
[22] A. Manoharan, K.M. Begam, V.R. Aparow, D. Sooriamoorthy, Artificial Neural Networks, Gradient Boosting and Support Vector Machines for electric vehicle battery state estimation: A review, J. Energy Storage. 55 (2022), 105384, https://doi.org/10.1016/j.est.2022.105384.
[23] R. Xiong, Y. Sun, C. Wang, J. Tian, X. Chen, H. Li, Q. Zhang, A data-driven method for extracting aging features to accurately predict the battery health, Energy Storage Mater 57 (2023) 460–470, https://doi.org/10.1016/j.ensm.2023.02.034.
[24] K. Luo, X. Chen, H. Zheng, Z. Shi, A review of deep learning approach to predicting the state of health and state of charge of lithium-ion batteries, J. Energy Chem. 74 (2022) 159–173, https://doi.org/10.1016/j.jechem.2022.06.049.
[25] Y. LeCun, Y. Bengio, G. Hinton, Deep learning, Nature 521 (2015) 436–444, https://doi.org/10.1038/nature14539.
[26] A. Aitio, D.A. Howey, Predicting battery end of life from solar off-grid system field data using machine learning, Joule 5 (2021) 3204–3220, https://doi.org/10.1016/j.joule.2021.11.006.
[27] K. Li, P. Zhou, Y. Lu, X. Han, X. Li, Y. Zheng, Battery life estimation based on cloud data for electric vehicles, J. Power Sources. 468 (2020), 228192, https://doi.org/10.1016/j.jpowsour.2020.228192.
[28] B. Wu, W.D. Widanage, S. Yang, X. Liu, Battery digital twins: Perspectives on the fusion of models, data and artificial intelligence for smart battery management systems, Energy AI 1 (2020), 100016, https://doi.org/10.1016/j.egyai.2020.100016.
[29] Y. Zhao, Z. Wang, Z.J.M. Shen, F. Sun, Assessment of battery utilization and energy consumption in the large-scale development of urban electric vehicles, Proc. Natl. Acad. Sci. U. S. A. (2021) 118, https://doi.org/10.1073/pnas.2017318118.
[30] C. Chen, R. Xiong, R. Yang, H. Li, A novel data-driven method for mining battery open-circuit voltage characterization, Green Energy Intell. Transp. 1 (2022), 100001, https://doi.org/10.1016/j.geits.2022.100001.
[31] L. Ma, C. Hu, F. Cheng, State of Charge and State of Energy Estimation for Lithium-Ion Batteries Based on a Long Short-Term Memory Neural Network, J. Energy Storage. 37 (2021), 102440, https://doi.org/10.1016/j.est.2021.102440.
[32] F. Yang, S. Zhang, W. Li, Q. Miao, State-of-charge estimation of lithium-ion batteries using LSTM and UKF, Energy 201 (2020), 117664, https://doi.org/10.1016/j.energy.2020.117664.
[33] J. Tian, R. Xiong, W. Shen, J. Lu, State-of-charge estimation of LiFePO4 batteries in electric vehicles: A deep-learning enabled approach, Appl. Energy. 291 (2021), 116812, https://doi.org/10.1016/j.apenergy.2021.116812.
[34] C. Hu, L. Ma, S. Guo, G. Guo, Z. Han, Deep learning enabled state-of-charge estimation of LiFePO4 batteries: A systematic validation on state-of-the-art charging protocols, Energy 246 (2022), 123404, https://doi.org/10.1016/j.energy.2022.123404.
[35] J. Tian, R. Xiong, W. Shen, F. Sun, Electrode ageing estimation and open circuit voltage reconstruction for lithium ion batteries, Energy Storage Mater 37 (2021) 283–295, https://doi.org/10.1016/j.ensm.2021.02.018.
[36] J. Wu, X. Cui, J. Meng, J. Peng, M. Lin, Data-Driven Transfer-Stacking based State of Health Estimation for Lithium-Ion Batteries, IEEE Trans. Ind. Electron. (2023) 1–11, https://doi.org/10.1109/TIE.2023.3247735.
[37] Z. Huang, L. Sugiarto, Y. Lu, Feature–target pairing in machine learning for battery health diagnosis and prognosis: a critical review, EcoMat 5 (2023) 1–15, https://doi.org/10.1002/eom2.12345.
[38] D.P. Finegan, J. Zhu, X. Feng, M. Keyser, M. Ulmefors, W. Li, M.Z. Bazant, S. J. Cooper, The Application of Data-Driven Methods and Physics-Based Learning for Improving Battery Safety, Joule 5 (2021) 316–329, https://doi.org/10.1016/j.joule.2020.11.018.
[39] Q. Yu, C. Wang, J. Li, R. Xiong, M. Pecht, Challenges and outlook for lithium-ion battery fault diagnosis methods from the laboratory to real world applications, eTransportation 17 (2023), 100254, https://doi.org/10.1016/j.etran.2023.100254.
[40] J. Tian, R. Xiong, W. Shen, A review on state of health estimation for lithium ion batteries in photovoltaic systems, eTransportation 2 (2019), 100028, https://doi.org/10.1016/j.etran.2019.100028.
[41] V. Sulzer, P. Mohtat, A. Aitio, S. Lee, Y.T. Yeh, F. Steinbacher, M.U. Khan, J. W. Lee, J.B. Siegel, A.G. Stefanopoulou, D.A. Howey, The challenge and opportunity of battery lifetime prediction from field data, Joule 5 (2021) 1934–1955, https://doi.org/10.1016/j.joule.2021.06.005.
[42] P. Kollmeyer, Panasonic 18650PF Li-ion battery data, Mendeley Data 1 (2018).
[43] P. Kollmeyer, C. Vidal, M. Naguib, M. Skells, LG 18650HG2 Li-ion battery data and example deep neural network xEV SOC estimator script, Mendeley Data 3 (2020).
[44] P. Kollmeyer, M. Skells, Turnigy graphene 5000mAh 65C Li-ion battery data, Mendeley Data 1 (2020).
[45] CALCE, CALCE LFP dataset, 2023 n.d. https://web.calce.umd.edu/batteries/data.htm#A123.
[46] F. Chollet, Deep learning with Python, Simon and Schuster, 2017.
[47] J. Tian, R. Xiong, J. Lu, C. Chen, W. Shen, Battery state-of-charge estimation amid dynamic usage with physics-informed deep learning, Energy Storage Mater 50 (2022) 718–729, https://doi.org/10.1016/j.ensm.2022.06.007.
[48] S. Ruder, An overview of gradient descent optimization algorithms (2016) 1–14. http://arxiv.org/abs/1609.04747.
[49] P.M. Attia, A. Grover, N. Jin, K.A. Severson, T.M. Markov, Y.H. Liao, M.H. Chen, B. Cheong, N. Perkins, Z. Yang, P.K. Herring, M. Aykol, S.J. Harris, R.D. Braatz, S. Ermon, W.C. Chueh, Closed-loop optimization of fast-charging protocols for

batteries with machine learning, Nature 578 (2020) 397–402, https://doi.org/10.1038/s41586-020-1994-5.
[50] E. Chemali, P.J. Kollmeyer, M. Preindl, A. Emadi, State-of-charge estimation of Li-ion batteries using deep neural networks: A machine learning approach, J. Power Sources. 400 (2018) 242–255, https://doi.org/10.1016/j.jpowsour.2018.06.104.
[51] D.N.T. How, M.A. Hannan, M.S.H. Lipu, K.S.M. Sahari, P.J. Ker, K.M. Muttaqi, State-of-Charge Estimation of Li-Ion Battery in Electric Vehicles: A Deep Neural Network Approach, IEEE Trans. Ind. Appl. 56 (2020) 5565–5574, https://doi.org/10.1109/TIA.2020.3004294.
[52] M.A. Hannan, M.S.H. Lipu, A. Hussain, M.H. Saad, A. Ayob, Neural network approach for estimating state of charge of lithium-ion battery using backtracking search algorithm, IEEE Access 6 (2018) 10069–10079, https://doi.org/10.1109/ACCESS.2018.2797976.
[53] D. Andre, M. Meiler, K. Steiner, C. Wimmer, T. Soczka-Guth, D.U. Sauer, Characterization of high-power lithium-ion batteries by electrochemical impedance spectroscopy. I. Experimental investigation, J. Power Sources. 196 (2011) 5334–5341, https://doi.org/10.1016/j.jpowsour.2010.12.102.
[54] M.S.H. Lipu, M.A. Hannan, A. Hussain, M.H.M. Saad, A. Ayob, K.M. Muttaqi, Lithium-ion Battery State of Charge Estimation Method Using Optimized Deep Recurrent Neural Network Algorithm, in: 2019 IEEE Ind. Appl. Soc. Annu. Meet, IAS, 2019, pp. 1–9, https://doi.org/10.1109/IAS.2019.8912322, 2019.
[55] S. Hochreiter, J. Schmidhuber, Long Short-Term Memory, Neural Comput 9 (1997) 1735–1780, https://doi.org/10.1162/neco.1997.9.8.1735.
[56] G. Van Houdt, C. Mosquera, G. Nápoles, A review on the long short-term memory model, Artif. Intell. Rev. 53 (2020) 5929–5955, https://doi.org/10.1007/s10462-020-09838-1.
[57] A. Garg, M. Agarwal, Machine Translation: A Literature Review, (2018). http://arxiv.org/abs/1901.01122.
[58] R. Jin, Z. Chen, K. Wu, M. Wu, X. Li, R. Yan, Bi-LSTM-Based Two-Stream Network for Machine Remaining Useful Life Prediction, IEEE Trans. Instrum. Meas. 71 (2022), https://doi.org/10.1109/TIM.2022.3167778.
[59] Y. Zhang, R. Xiong, H. He, M.G. Pecht, Long short-term memory recurrent neural network for remaining useful life prediction of lithium-ion batteries, IEEE Trans. Veh. Technol. 67 (2018) 5695–5705, https://doi.org/10.1109/TVT.2018.2805189.
[60] K. Cho, B. Van Merriënboer, C. Gulcehre, D. Bahdanau, F. Bougares, H. Schwenk, Y. Bengio, Learning phrase representations using RNN encoder-decoder for statistical machine translation, in: EMNLP 2014 - 2014 Conf. Empir. Methods Nat. Lang. Process. Proc. Conf, 2014, pp. 1724–1734, https://doi.org/10.3115/v1/d14-1179.
[61] J. Chung, C. Gulcehre, K. Cho, Y. Bengio, Empirical Evaluation of Gated Recurrent Neural Networks on Sequence Modeling (2014) 1–9. http://arxiv.org/abs/1412.3555.
[62] E. Chemali, P.J. Kollmeyer, M. Preindl, R. Ahmed, A. Emadi, Long Short-Term Memory Networks for Accurate State-of-Charge Estimation of Li-ion Batteries, IEEE Trans. Ind. Electron. 65 (2018) 6730–6739, https://doi.org/10.1109/TIE.2017.2787586.
[63] X. Ren, S. Liu, X. Yu, X. Dong, A method for state-of-charge estimation of lithium-ion batteries based on PSO-LSTM, Energy 234 (2021), 121236, https://doi.org/10.1016/j.energy.2021.121236.
[64] F. Yang, W. Li, C. Li, Q. Miao, State-of-charge estimation of lithium-ion batteries based on gated recurrent neural network, Energy 175 (2019) 66–75, https://doi.org/10.1016/j.energy.2019.03.059.
[65] M.A. Hannan, D.N.T. How, M. Bin Mansor, M.S. Hossain Lipu, P. Ker, K. Muttaqi, State-of-Charge Estimation of Li-ion Battery Using Gated Recurrent Unit with One-Cycle Learning Rate Policy, IEEE Trans. Ind. Appl. 57 (2021) 2964–2971, https://doi.org/10.1109/TIA.2021.3065194.
[66] F. Yang, X. Song, F. Xu, K.L. Tsui, State-of-Charge Estimation of Lithium-Ion Batteries via Long Short-Term Memory Network, IEEE Access 7 (2019) 53792–53799, https://doi.org/10.1109/ACCESS.2019.2912803.
[67] C. Bian, H. He, S. Yang, Stacked bidirectional long short-term memory networks for state-of-charge estimation of lithium-ion batteries, Energy 191 (2020), 116538, https://doi.org/10.1016/j.energy.2019.116538.
[68] Z. Zhang, Z. Dong, H. Lin, Z. He, M. Wang, Y. He, X. Gao, M. Gao, An Improved Bidirectional Gated Recurrent Unit Method for Accurate State-of-Charge Estimation, IEEE Access 9 (2021) 11252–11263, https://doi.org/10.1109/ACCESS.2021.3049944.
[69] D.N.T. How, M.A. Hannan, S. Member, M.S.H. Lipu, P.J. Ker, M. Mansor, K.S. M. Sahari, S. Member, K.M. Muttaqi, S. Member, SOC Estimation Using Deep Bidirectional Gated Recurrent Units With Tree Parzen Estimator Hyperparameter Optimization FLOPS GS RS, IEEE Trans. Ind. Appl. 58 (2022) 6629–6638, https://doi.org/10.1109/TIA.2022.3180282.
[70] L. Ma, Z. Wang, F. Yang, Y. Cheng, C. Lu, L. Tao, T. Zhou, Robust state of charge estimation based on a sequence-to-sequence mapping model with process information, J. Power Sources. 474 (2020), 228691, https://doi.org/10.1016/j.jpowsour.2020.228691.
[71] K. Yang, Y. Tang, S. Zhang, Z. Zhang, A deep learning approach to state of charge estimation of lithium-ion batteries based on dual-stage attention mechanism, Energy 244 (2022), 123233, https://doi.org/10.1016/j.energy.2022.123233.
[72] S. Li, W. Li, C. Cook, C. Zhu, Y. Gao, Independently recurrent neural network (indrnn): Building a longer and deeper rnn, in: Proc. IEEE Conf. Comput. Vis, Pattern Recognit, 2018, pp. 5457–5466.
[73] P. Venugopal, T. Vigneswaran, S. Reka, S, State of Charge Estimation of Lithium Batteries in Electric Vehicles Using IndRNN, IETE J. Res. (2021), https://doi.org/10.1080/03772063.2021.1906770.
[74] X. Feng, J. Chen, Z. Zhang, S. Miao, Q. Zhu, State-of-charge estimation of lithium-ion battery based on clockwork recurrent neural network, Energy 236 (2021), 121360, https://doi.org/10.1016/j.energy.2021.121360.
[75] J. Koutnik, K. Greff, F. Gomez, J. Schmidhuber, A clockwork rnn, in: Int. Conf. Mach. Learn., PMLR, 2014, pp. 1863–1871.
[76] C. Hu, F. Cheng, L. Ma, B. Li, State of Charge Estimation for Lithium-Ion Batteries Based on TCN-LSTM Neural Networks, J. Electrochem. Soc. (2022), https://doi.org/10.1149/1945-7111/ac5cf2.
[77] Z. Xi, R. Wang, Y. Fu, C. Mi, Accurate and reliable state of charge estimation of lithium ion batteries using time-delayed recurrent neural networks through the identification of overexcited neurons, Appl. Energy. 305 (2022), 117962, https://doi.org/10.1016/j.apenergy.2021.117962.
[78] Y. LeCun, B. Boser, J. Denker, D. Henderson, R. Howard, W. Hubbard, L. Jackel, Handwritten digit recognition with a back-propagation network, Adv. Neural Inf. Process. Syst. 2 (1989).
[79] S. Kiranyaz, O. Avci, O. Abdeljaber, T. Ince, M. Gabbouj, D.J. Inman, 1D convolutional neural networks and applications: A survey, Mech. Syst. Signal Process 151 (2021), 107398, https://doi.org/10.1016/j.ymssp.2020.107398.
[80] M.A. Hannan, D.N.T. How, M.S. Hossain Lipu, P.J. Ker, Z.Y. Dong, M. Mansur, F. Blaabjerg, SOC Estimation of Li-ion Batteries with Learning Rate-Optimized Deep Fully Convolutional Network, IEEE Trans. Power Electron. 36 (2021) 7349–7353, https://doi.org/10.1109/TPEL.2020.3041876.
[81] S. Guo, L. Ma, A comparative study of different deep learning algorithms for lithium-ion batteries on state-of-charge estimation, Energy 263 (2023), 125872, https://doi.org/10.1016/j.energy.2022.125872.
[82] C. Lea, M.D. Flynn, R. Vidal, A. Reiter, G.D. Hager, Temporal Convolutional Networks for Action Segmentation and Detection, in: 2017 IEEE Conf. Comput. Vis. Pattern Recognit, IEEE, 2017, pp. 1003–1012, https://doi.org/10.1109/CVPR.2017.113.
[83] C. Lea, R. Vidal, A. Reiter, G.D. Hager, Temporal convolutional networks: A unified approach to action segmentation, in: Comput. Vision–ECCV 2016 Work. Amsterdam, Netherlands, Oct. 8-10 15-16, 2016, Proceedings, Part III 14, Springer, 2016, pp. 47–54.
[84] A. van den Oord, S. Dieleman, H. Zen, K. Simonyan, O. Vinyals, A. Graves, N. Kalchbrenner, A. Senior, K. Kavukcuoglu, WaveNet: A Generative Model for Raw Audio (2016) 1–15. http://arxiv.org/abs/1609.03499.
[85] K. He, X. Zhang, S. Ren, J. Sun, Deep residual learning for image recognition, in: Proc. IEEE Comput. Soc. Conf. Comput. Vis. Pattern Recognit, 2016, pp. 770–778, https://doi.org/10.1109/CVPR.2016.90, 2016–Decem.
[86] A. Bhattacharjee, A. Verma, S. Mishra, T.K. Saha, Estimating State of Charge for xEV Batteries Using 1D Convolutional Neural Networks and Transfer Learning, IEEE Trans. Veh. Technol. 70 (2021) 3123–3135, https://doi.org/10.1109/TVT.2021.3064287.
[87] Q. Gong, P. Wang, Z. Cheng, J. Zhang, A Method for Estimating State of Charge of Lithium-Ion Batteries Based on Deep Learning, J. Electrochem. Soc. 168 (2021), 110532, https://doi.org/10.1149/1945-7111/ac3719.
[88] M. Zhao, M. Kang, B. Tang, M. Pecht, Multiple Wavelet Coefficients Fusion in Deep Residual Networks for Fault Diagnosis, IEEE Trans. Ind. Electron. 66 (2019) 4696–4706, https://doi.org/10.1109/TIE.2018.2866050.
[89] Y. Lu, C.Z. Zhao, J.Q. Huang, Q. Zhang, The timescale identification decoupling complicated kinetic processes in lithium batteries, Joule 6 (2022) 1172–1198, https://doi.org/10.1016/j.joule.2022.05.005.
[90] X. Song, F. Yang, D. Wang, K.L. Tsui, Combined CNN-LSTM Network for State-of-Charge Estimation of Lithium-Ion Batteries, IEEE Access 7 (2019) 88894–88902, https://doi.org/10.1109/ACCESS.2019.2926517.
[91] C. Bian, S. Yang, Q. Miao, Cross-Domain State-of-Charge Estimation of Li-Ion Batteries Based on Deep Transfer Neural Network With Multiscale Distribution Adaptation, IEEE Trans. Transp. Electrif. 7 (2021) 1260–1270, https://doi.org/10.1109/TTE.2020.3041604.
[92] J. Quionero-Candela, M. Sugiyama, A. Schwaighofer, N.D. Lawrence, Dataset shift in machine learning, The MIT Press, 2009.
[93] W. Li, R. Huang, J. Li, Y. Liao, Z. Chen, G. He, R. Yan, K. Gryllias, A perspective survey on deep transfer learning for fault diagnosis in industrial scenarios: Theories, applications and challenges, Mech. Syst. Signal Process. 167 (2022), 108487, https://doi.org/10.1016/j.ymssp.2021.108487.
[94] S.J. Pan, Q. Yang, A Survey on Transfer Learning, IEEE Trans. Knowl. Data Eng. 22 (2010) 1345–1359, https://doi.org/10.1109/TKDE.2009.191.
[95] Y. Lei, B. Yang, X. Jiang, F. Jia, N. Li, A.K. Nandi, Applications of machine learning to machine fault diagnosis: A review and roadmap, Mech. Syst. Signal Process. 138 (2020), 106587, https://doi.org/10.1016/j.ymssp.2019.106587.
[96] Y. Liu, X. Shu, H. Yu, J. Shen, Y. Zhang, Y. Liu, Z. Chen, State of charge prediction framework for lithium-ion batteries incorporating long short-term memory network and transfer learning, J. Energy Storage. 37 (2021), 102494, https://doi.org/10.1016/j.est.2021.102494.
[97] Z. Zhao, Q. Zhang, X. Yu, C. Sun, S. Wang, R. Yan, X. Chen, Applications of Unsupervised Deep Transfer Learning to Intelligent Fault Diagnosis: A Survey and Comparative Study, IEEE Trans. Instrum. Meas. 70 (2021) 1–28, https://doi.org/10.1109/TIM.2021.3116309.
[98] T. Han, Z. Wang, H. Meng, End-to-end capacity estimation of Lithium-ion batteries with an enhanced long short-term memory network considering domain adaptation, J. Power Sources. 520 (2022), 230823, https://doi.org/10.1016/j.jpowsour.2021.230823.
[99] K.M. Borgwardt, A. Gretton, M.J. Rasch, H.P. Kriegel, B. Schölkopf, A.J. Smola, Integrating structured biological data by Kernel Maximum Mean Discrepancy, Bioinformatics 22 (2006) 49–57, https://doi.org/10.1093/bioinformatics/btl242.

[100] J. Lu, R. Xiong, J. Tian, C. Wang, F. Sun, Deep learning to estimate lithium-ion battery state of health without additional degradation experiments, Nat. Commun. 14 (2023) 2760, https://doi.org/10.1038/s41467-023-38458-w.
[101] Z. Meng, K.A. Agyeman, X. Wang, Lithium-Ion Battery State of Charge Estimation with Adaptability to Changing Conditions, IEEE Trans. Energy Convers. PP (2023) 1–11, https://doi.org/10.1109/TEC.2023.3285405.
[102] I. Oyewole, A. Chehade, Y. Kim, A controllable deep transfer learning network with multiple domain adaptation for battery state-of-charge estimation, Appl. Energy. 312 (2022), 118726, https://doi.org/10.1016/j.apenergy.2022.118726.
[103] S. Zhang, C. Zhang, S. Jiang, X. Zhang, A comparative study of different adaptive extended/unscented Kalman filters for lithium-ion battery state-of-charge estimation, Energy 246 (2022), 123423, https://doi.org/10.1016/j.energy.2022.123423.
[104] H. Yu, L. Zhang, W. Wang, S. Li, S. Chen, S. Yang, J. Li, X. Liu, State of charge estimation method by using a simplified electrochemical model in deep learning framework for lithium-ion batteries, Energy 278 (2023), 127846, https://doi.org/10.1016/j.energy.2023.127846.
[105] Y. Cheng, X. Zhang, X. Wang, J. Li, Battery State of Charge Estimation Based on Composite Multiscale Wavelet Transform, Energies 15 (2022) 2064, https://doi.org/10.3390/en15062064.
[106] M. Ragone, V. Yurkiv, A. Ramasubramanian, B. Kashir, F. Mashayek, Data driven estimation of electric vehicle battery state-of-charge informed by automotive simulations and multi-physics modeling, J. Power Sources. 483 (2021), 229108, https://doi.org/10.1016/j.jpowsour.2020.229108.
[107] M. Dubarry, D. Beck, Big data training data for artificial intelligence-based Li-ion diagnosis and prognosis, J. Power Sources. 479 (2020), 228806, https://doi.org/10.1016/j.jpowsour.2020.228806.
[108] M. Dubarry, N. Costa, D. Matthews, Data-driven direct diagnosis of Li-ion batteries connected to photovoltaics, Nat. Commun. 14 (2023) 3138, https://doi.org/10.1038/s41467-023-38895-7.
[109] N. Gan, Z. Sun, Z. Zhang, S. Xu, P. Liu, Z. Qin, Data-Driven Fault Diagnosis of Lithium-Ion Battery Overdischarge in Electric Vehicles, IEEE Trans. Power Electron. 37 (2021) 4575–4588.
[110] M.A. Hannan, D.N.T. How, M.S.H. Lipu, M. Mansor, P.J. Ker, Z.Y. Dong, K.S. M. Sahari, S.K. Tiong, K.M. Muttaqi, T.M.I. Mahlia, F. Blaabjerg, Deep learning approach towards accurate state of charge estimation for lithium-ion batteries using self-supervised transformer model, Sci. Rep. 11 (2021) 19541, https://doi.org/10.1038/s41598-021-98915-8.
[111] L. Ma, T. Zhang, Deep learning-based battery state of charge estimation: Enhancing estimation performance with unlabelled training samples, J. Energy Chem. (2023), https://doi.org/10.1016/j.jechem.2023.01.036.
[112] R. Xiong, J. Tian, W. Shen, J. Lu, F. Sun, Semi-supervised estimation of capacity degradation for lithium ion batteries with electrochemical impedance spectroscopy, J. Energy Chem. 76 (2023) 404–413, https://doi.org/10.1016/j.jechem.2022.09.045.
[113] V. Sulzer, S.G. Marquis, R. Timms, M. Robinson, S.J. Chapman, Python battery mathematical modelling (PyBaMM), J. Open Res. Softw 9 (2021).
[114] W. Wang, J. Wang, J. Tian, J. Lu, R. Xiong, Application of Digital Twin in Smart Battery Management Systems, Chinese J. Mech. Eng. 34 (2021) 57, https://doi.org/10.1186/s10033-021-00577-0.
[115] J. Tian, R. Xiong, W. Shen, J. Lu, Data-driven battery degradation prediction: Forecasting voltage-capacity curves using one-cycle data, EcoMat (2022) 1–12, https://doi.org/10.1002/eom2.12213.
[116] C.-W. Hsu, R. Xiong, N.-Y. Chen, J. Li, N.-T. Tsou, Deep neural network battery life and voltage prediction by using data of one cycle only, Appl. Energy. 306 (2022), 118134, https://doi.org/10.1016/j.apenergy.2021.118134.
[117] J. Hong, D. Lee, E.R. Jeong, Y. Yi, Towards the swift prediction of the remaining useful life of lithium-ion batteries with end-to-end deep learning, Appl. Energy. 278 (2020), 115646, https://doi.org/10.1016/j.apenergy.2020.115646.
[118] D. Yang, J. Liu, Y. Wang, M. Chen, B. Zhang, Y. Li, State-of-Charge Estimation Using a Self-adaptive Noise Extended Kalman Filter For Lithium Batteries, (2014).
[119] X. Li, J. Jiang, C. Zhang, L.Y. Wang, L. Zheng, Robustness of SOC Estimation Algorithms for EV Lithium-Ion Batteries against Modeling Errors and Measurement Noise, Math. Probl. Eng. (2015) 1–14, https://doi.org/10.1155/2015/719490, 2015.
[120] M.S. Reza, M.A. Hannan, P.J. Ker, M. Mansor, M.S.H. Lipu, M.J. Hossain, T.M. I. Mahlia, Uncertainty parameters of battery energy storage integrated grid and their modeling approaches: A review and future research directions, J. Energy Storage. 68 (2023), 107698, https://doi.org/10.1016/j.est.2023.107698.
[121] E. Hüllermeier, W. Waegeman, Aleatoric and epistemic uncertainty in machine learning: an introduction to concepts and methods, Mach. Learn. 110 (2021) 457–506, https://doi.org/10.1007/s10994-021-05946-3.
[122] Y. Gal, Z. Ghahramani, Dropout as a Bayesian Approximation: Representing Model Uncertainty in Deep Learning, in: M.F. Balcan, K.Q. Weinberger (Eds.), Proc. 33rd Int. Conf. Mach. Learn., PMLR, New York, New York, USA, 2016, pp. 1050–1059.
[123] T. Han, Y.F. Li, Out-of-distribution detection-assisted trustworthy machinery fault diagnosis approach with uncertainty-aware deep ensembles, Reliab. Eng. Syst. Saf. 226 (2022), 108648, https://doi.org/10.1016/j.ress.2022.108648.
[124] G. Palmer, S. Du, A. Politowicz, J.P. Emory, X. Yang, A. Gautam, G. Gupta, Z. Li, R. Jacobs, D. Morgan, Calibration after bootstrap for accurate uncertainty quantification in regression models, Npj Comput. Mater. 8 (2022) 1–9, https://doi.org/10.1038/s41524-022-00794-8.
[125] J. Tian, R. Xiong, W. Shen, J. Lu, F. Sun, Flexible battery state of health and state of charge estimation using partial charging data and deep learning, Energy Storage Mater 51 (2022) 372–381, https://doi.org/10.1016/j.ensm.2022.06.053.
[126] M. Crawshaw, Multi-Task Learning with Deep Neural Networks: A Survey, (2020). http://arxiv.org/abs/2009.09796.
[127] J. Tian, R. Xiong, W. Shen, J. Lu, X.-G. Yang, Deep neural network battery charging curve prediction using 30 points collected in 10 min, Joule 5 (2021) 1521–1534, https://doi.org/10.1016/j.joule.2021.05.012.
[128] M.S. Hosen, A quick battery charging curve prediction by artificial neural network, Patterns 2 (2021), 100338, https://doi.org/10.1016/j.patter.2021.100338.
[129] Y. Duan, J. Tian, J. Lu, C. Wang, W. Shen, R. Xiong, Deep neural network battery impedance spectra prediction by only using constant-current curve, Energy Storage Mater 41 (2021) 24–31, https://doi.org/10.1016/j.ensm.2021.05.047.
[130] J. Tian, R. Xiong, C. Chen, C. Wang, W. Shen, F. Sun, Simultaneous prediction of impedance spectra and state for lithium-ion batteries from short-term pulses, Electrochim. Acta. 449 (2023), 142218, https://doi.org/10.1016/j.electacta.2023.142218.
[131] X. Tang, X. Lai, Q. Liu, Y. Zheng, Y. Zhou, Y. Ma, F. Gao, Predicting battery impedance spectra from 10-second pulse tests under 10 Hz sampling rate, iScience 26 (2023), 106821, https://doi.org/10.1016/j.isci.2023.106821.
[132] X. Wang, Y. Kou, B. Wang, Z. Jiang, X. Wei, H. Dai, Fast Calculation of Broadband Battery Impedance Spectra Based on S Transform of Step Disturbance and Response, IEEE Trans. Transp. Electrif. 8 (2022) 3659–3672, https://doi.org/10.1109/TTE.2022.3153680.
[133] X. Wang, X. Wei, J. Zhu, H. Dai, Y. Zheng, X. Xu, Q. Chen, A review of modeling, acquisition, and application of lithium-ion battery impedance for onboard battery management, eTransportation 7 (2021) 100093, https://doi.org/10.1016/j.etran.2020.100093.
[134] X. Du, J. Meng, J. Peng, Hybrid Pseudorandom Sequence for Broadband Impedance Measurements of Lithium-Ion Batteries, IEEE Trans. Ind. Electron. 70 (2023) 6856–6864, https://doi.org/10.1109/TIE.2022.3201347.
[135] X. Du, J. Meng, J. Peng, Y. Liu, A Novel Lithium-Ion Battery Impedance Fast Measurement Method With Enhanced Excitation Signal, IEEE Trans. Ind. Electron. 70 (2023) 12322–12330, https://doi.org/10.1109/TIE.2023.3234127.
[136] X. Lin, Real-Time Prediction of Anode Potential in Li-Ion Batteries Using Long Short-Term Neural Networks for Lithium Plating Prevention, J. Electrochem. Soc. 166 (2019) A1893–A1904, https://doi.org/10.1149/2.0621910jes.
[137] W. Li, J. Zhang, F. Ringbeck, D. Jöst, L. Zhang, Z. Wei, D.U. Sauer, Physics-informed neural networks for electrode-level state estimation in lithium-ion batteries, J. Power Sources. 506 (2021), 230034, https://doi.org/10.1016/j.jpowsour.2021.230034.
[138] Y. Lu, X. Han, Z. Chu, X. Feng, Y. Qin, M. Ouyang, L. Lu, A decomposed electrode model for real-time anode potential observation of lithium-ion batteries, J. Power Sources. 513 (2021), 230529, https://doi.org/10.1016/j.jpowsour.2021.230529.
[139] S. Dey, Y. Shi, K. Smith, A. Colclasure, X. Li, From Battery Cell to Electrodes: Real-Time Estimation of Charge and Health of Individual Battery Electrodes, IEEE Trans. Ind. Electron. 67 (2020) 2167–2175, https://doi.org/10.1109/TIE.2019.2907514.
[140] Z. Wei, J. Hu, H. He, Y. Yu, J. Marco, Embedded Distributed Temperature Sensing Enabled Multistate Joint Observation of Smart Lithium-Ion Battery, IEEE Trans. Ind. Electron. 70 (2023) 555–565, https://doi.org/10.1109/TIE.2022.3146503.
[141] B. Jiang, S. Tao, X. Wang, J. Zhu, X. Wei, H. Dai, Mechanics-based state of charge estimation for lithium-ion pouch battery using deep learning technique, Energy 278 (2023), 127890, https://doi.org/10.1016/j.energy.2023.127890.
[142] Z. Wei, J. Zhao, H. He, G. Ding, H. Cui, L. Liu, Future smart battery and management: Advanced sensing from external to embedded multi-dimensional measurement, J. Power Sources. 489 (2021), 229462, https://doi.org/10.1016/j.jpowsour.2021.229462.
[143] M. Dubarry, D. Howey, B. Wu, Enabling battery digital twins at the industrial scale, Joule 7 (2023) 1134–1144, https://doi.org/10.1016/j.joule.2023.05.005.
[144] W. Li, M. Rentemeister, J. Badeda, D. Jöst, D. Schulte, D.U. Sauer, Digital twin for battery systems: Cloud battery management system with online state-of-charge and state-of-health estimation, J. Energy Storage. 30 (2020), 101557, https://doi.org/10.1016/j.est.2020.101557.
[145] A. Mondal, A. Routray, S. Puravankara, Parameter identification and co-estimation of state-of-charge of Li-ion battery in real-time on Internet-of-Things platform, J. Energy Storage. 51 (2022), 104370, https://doi.org/10.1016/j.est.2022.104370.
[146] J.M. Reniers, D.A. Howey, Digital twin of a MWh-scale grid battery system for efficiency and degradation analysis, Appl. Energy. 336 (2022), 120774, https://doi.org/10.1016/j.apenergy.2023.120774.
[147] X. Tang, Y. Zhou, F. Gao, X. Lai, Joint estimation of state-of-charge and state-of-health for all cells in the battery pack using "leader-follower" strategy, eTransportation 15 (2022), 100213, https://doi.org/10.1016/j.etran.2022.100213.
[148] S. Zhang, X. Zhang, A novel low-complexity state-of-energy estimation method for series-connected lithium-ion battery pack based on "representative cell" selection and operating mode division, J. Power Sources. 518 (2022), 230732, https://doi.org/10.1016/j.jpowsour.2021.230732.
[149] F. An, W. Zhang, B. Sun, J. Jiang, X. Fan, A novel state-of-energy simplified estimation method for lithium-ion battery pack based on prediction and

representative cells, J. Energy Storage. 63 (2023), 107083, https://doi.org/10.1016/j.est.2023.107083.
[150] Q. Yu, Y. Huang, A. Tang, C. Wang, W. Shen, OCV-SOC-Temperature Relationship Construction and State of Charge Estimation for a Series– Parallel Lithium-Ion Battery Pack, IEEE Trans. Intell. Transp. Syst. 24 (2023) 6362–6371, https://doi.org/10.1109/tits.2023.3252164.
[151] X. Tang, F. Gao, X. Lai, Compressing and reconstructing the voltage data for lithium-ion batteries using model migration and un-equidistant sampling techniques, eTransportation 13 (2022), 100186, https://doi.org/10.1016/j.etran.2022.100186.